國立臺灣大學電機資訊學院電信工程學研究所

博士論文

Graduate Institute of Communication Engineering
College of Electrical Engineering and Computer Science
National Taiwan University

Doctoral Dissertation

背覆平板共平面波導饋入印刷天線之設計

Design of Printed Antenna Fed by Coplanar Waveguide With Backing Plate

呂彥儒

Yen-Ju Lu

指導教授：許博文 博士

Advisor: Dr. Powen Hsu

中華民國 103 年 7 月

July, 2014

國立臺灣大學博士學位論文
口試委員會審定書

背覆平板共平面波導饋入印刷天線之設計
Design of Printed Antenna Fed by Coplanar Waveguide With Backing Plate

本論文係呂彥儒君（D98942010）在國立臺灣大學電信工程學研究所完成之博士學位論文，於民國一百零三年七月二十五日承下列考試委員審查通過及口試及格，特此證明

口試委員：許博文（簽名）

（指導教授）

鄭士康　楊志銘

陳士元　毛紹綱

李學智

所　長　吳宗霖（簽名）

誌謝

本論文的完成，首先得感謝許博文教授的耐心指導與栽培。在學術研究上，許教授給了我很大的自由發揮空間，讓我能夠盡情地揮灑創意，當我遇到問題時，許教授總能精闢的分析且給我許多建議，令我獲益良多，當我遇到困難的時候，教授總是能適時地給予幫助，此外，許教授獨到的人生哲學也深深地讓我景仰與佩服。其次，我要特別感謝陳士元教授從我進實驗室開始就教導我很多專業的知識，當我研究上遇到困難時也給予我非常有幫助的建議。感謝口試委員李學智教授、鄭士康教授、楊成發教授以及毛紹綱教授，委員們的寶貴意見使本論文更臻完備。

感謝澤旻學長、儷憲學長、宜峰學長、小高、良昱、詩家、建伯、政豪、惠玲、立奇，與你們討論總是可以讓我豁然開朗。感謝許派的學長同學與學弟妹們：逸青、君朋、如弘、祐傑、奇軒、秉勳、凱程、忠侯、政隆、昱緯、兆祥、舷剛、訓斌、鈞涵、銘達、宗益、嘉隆、信毅、育名、威諭、閩豪、仲凱、韻儒、逸祥、永峰、昱宏，能夠與你們在天線研究上一起努力，是我的榮幸。感謝所有電波組教授、助理及季重儀先生，你們的努力與維護使得電波組更加茁壯。

感謝強哥在我遇到難題時總能給我寶貴的建議與非常正向的力量，使我能夠冷靜地處理並解決。感謝煥昇、易耕、煒恆和 soso，能夠認識你們，與你們天南地北地聊天、討論研究、談論時事以及吃美食時，我總是感到非常的輕鬆與自在，

你們的關心與鼓勵，是我在遇到挫折時還能夠繼續向前的動力，謝謝你們！

最後，感謝我的家人與幸甯，在這漫長的博士班生涯裡，你們全力地支持與體諒，讓我能無後顧之憂地完成學業，謝謝你們，謹以此論文獻給你們。

彥儒 2014.8.15

摘要

本論文提出背覆不同材質平板之共平面波導饋入印刷天線之設計，探討了印刷天線背覆空氣、導體和電磁能隙結構等三種不同材質時，天線特性的變化。首先探討的是在有及無背板導體時的共平面波導饋入印刷天線之設計，此設計可以在有及無背板導體時工作在相同的頻率而且擁有良好的天線輻射特性，主要是因為所提出的混和式設計在有及無背板導體時天線共振特性的改變已經被考量在內。因此，一個混和式設計可以被使用在無背板導體的無線通訊應用，同時在不更動其設計參數值，此設計也可以被用在需要背板導體時的應用。其次，一個縮小化的混和式設計也被提出和探討。接著，吾人提出一個增加阻抗頻寬的方法，有效地加大了混和式天線設計的阻抗頻寬，同時維持良好的天線輻射特性。

本論文下半部，主要探討背覆電磁能隙結構的共平面波導饋入印刷式槽偶極天線之設計，背覆電磁能隙結構與槽偶極天線之間的交互作用，使得背覆電磁能隙的設計與傳統共平面波導饋入槽偶極天線的設計有著顯著的不同，吾人於本論文詳述其差異並且提出一個完整的天線設計方法。

關鍵詞：背覆導體共平面波導、背覆導體槽線、共平面波導、電磁能隙結構、補釘天線、槽孔天線。

Abstract

Designs of printed antenna fed by coplanar waveguide (CPW) with different backing materials are presented in this dissertation. In the first half of this dissertation, hybrid designs of CPW-fed printed antenna with and without back conductor (BC) are presented. The hybrid designs can adapt themselves to the presence or absence of BC. First, the original hybrid design is proposed, analyzed, and designed. When BC is placed, the antenna is a conductor-backed CPW (CBCPW)-fed side plane patch antenna, while when BC is removed, the antenna becomes a CPW-fed slot dipole antenna. The antenna is designed to have the side plane patch and the slot dipole operate at the same frequency, so that it can adapt itself to the presence or absence of BC. In addition, miniaturization and bandwidth enhancement of the hybrid designs are presented, respectively. Compared with the original design, miniaturized design achieves roughly 40% reduction in size and the overlapping impedance bandwidth of the bandwidth-enhanced design is wider, approximately three times of the original design.

In the second half of this dissertation, design of an electromagnetic bandgap (EBG)-backed CPW-fed slot dipole antenna is presented. The antenna is formed by placing a CPW-fed slot dipole on the top of the EBG structure. It is found that the design considerations of the EBG-backed CPW-fed slot dipole are different from those

of the conventional CPW-fed slot dipole. This is because the propagation characteristics of the EBG-backed slotline utilized in the EBG-backed design are quite different from those of the slotline for the conventional design. By using the extracted propagation constant of the EBG-backed slotline, a detailed antenna design procedure is presented.

Index Terms—Conductor-backed coplanar waveguide (CBCPW), conductor-backed slotline (CBS), coplanar waveguide (CPW), electromagnetic bandgap (EBG) structures, patch antennas, slot antennas.

Contents

List of Figures

Chapter 3

List of Tables

Chapter 2

Chapter 3

Chapter 1

Introduction

1.1 MOTIVATION

Coplanar waveguide-fed printed antennas, such as slot antennas and patch antennas, have been widely used in wireless communications. For wireless communications, the antenna design becomes more stringent because a conductor plane would be needed to back the antenna for wireless communication system requirements, such as reduction of human body effect, improved heat sink capability and mechanical strength, and more space of placing components/devices under the antenna. When a coplanar waveguide-fed printed antenna is placed over the back conductor, the antenna performance could be degraded because the leakage problem in the conductor-backed coplanar waveguide arises and the characteristics of the antenna could be largely changed. This dissertation endeavors to seek for elegant designs of printed antenna fed by coplanar waveguide, which can adapt themselves to the presence or absence of back conductors. Thus whether the back conductor is used or not can depend upon the system requirements. In addition, this dissertation tries to analyze the coplanar waveguide-fed slot dipole antenna with back electromagnetic bandgap structure.

1.2 LITERATURE SURVEY

The coplanar waveguide (CPW) was proposed by C. P. Wen in 1969 [1]. It provides several advantages over the conventional microstripline, such as uniplanar structure, low radiation loss, low dispersion, ease of fabrication, and the ability of being easily integrated with active and passive devices without the need of via holes [2]. Therefore, it has become increasingly popular nowadays. The schematic of the CPW is shown in Fig. 1.1, where the dark and light gray areas represent the metal part and the dielectric substrate, respectively. The signal strip width *S*, gap width *G*, substrate thickness *h*, and dielectric constant ε_r determine the propagation constant and the characteristic impedance of CPW. To improve the mechanical strength of the substrate and the heat sink capability of the connected active circuits, a conducting plane, called back conductor (BC), is usually placed at the back of the CPW [2]. The CPW with BC turns into a conductor-backed CPW (CBCPW) or grounded CPW (GCPW). The schematic of the CBCPW is plotted in Fig. 1.2. The CBCPW has been widely used in various applications, for example, monolithic microwave integrated circuits [3], [4], filters [5]–[8], transitions [9]–[22], and sensors [23].

Early research on the CBCPW can be dated back to 1980s. Provided by Veyres and Hanna in 1980, analytical expressions for the effective dielectric constant and the

characteristic impedance of CBCPW are obtained by using conformal mapping technique [24]. In 1982, Shih and Itoh investigated the dispersion relation and characteristic impedance of CBCPW using spectral-domain technique [25]. Also, they indicated that CBCPW structure is a mixture of CPW and microstripline. When the gap width (G) increases for a fixed substrate thickness (h), the characteristics approach those of microstripline. On the other hand, as G is fixed and h increases, the behavior approaches the CPW case.

In the CBCPW, a parallel plate mode can exist in the dielectric-filled parallel-plate waveguide regions, which has a phase velocity that is less than that of the desired CPW mode and leaky waves then result as well as mode conversion at discontinuities [26]. Since the transverse electromagnetic (TEM) wave in the parallel-plate waveguide regions has zero cutoff frequency, there will always be some power leakage in the lateral direction for all frequencies [27], [28]. The quantitative descriptions of leakage is analyzed and provided in [27]–[29]. The leakage would increase the insertion loss of the CBCPW. It is observed that the leakage loss decreases with increasing substrate thickness [29]. However, using air bridges can suppress the parasitic mode (slotline mode) of CPW but cannot suppress the parallel-plate mode because the parallel-plate mode has the same symmetry as the CPW mode [30].

The CBCPW with finite-width top ground planes (side ground planes) is viewed as

three coupled microstriplines [31]. The schematic of CBCPW with side plane width (W_g) is plotted in Fig. 1.3. Compared with CBCPW with two semi-infinite-wide side ground planes, in the finite-width CBCPW, there is one more normal propagating mode, which is microstrip mode [31], called coplanar microstrip mode in [32] or microstrip-like (MSL) mode in [33]. The CPW mode and MSL mode have zero cutoff frequencies. Even for a simple, uniform, and symmetric finite-width CBCPW, the energy would couple from CPW mode to the MSL mode [31], not to mention that discontinuities in it happen [32]. The MSL mode not only takes energy away from the commonly launched CPW mode but also incurs the resonances of the side ground planes [33]–[36]. When resonances happen, large portion of the incident power would not be transmitted but rather be reflected and radiated and the resonant frequencies are predictable by employing the patch antenna theory [35], [36].

Several methods have been proposed to deal with the leakage problem in the CBCPW. First, the top and bottom conducting planes of the finite-width CBCPW are connected using metallic lateral walls [37]–[41] to eliminate the parallel-plate modes. This method maintains single CPW mode of propagation, if dimensions of the signal strip (S), gap width (G), and side plane width (W_g) are properly chosen [37]. The side plane width, which determines the cutoff frequency of the dielectric-filled rectangular waveguide mode, would be too small to maintain the advantages of CBCPW such as

heat sink capability, when the operating frequency is too high. A similar method uses via holes that short top and bottom conducting planes to suppress the parallel-plate modes [42]–[54]. In [46], Haydl found that placing via holes strategically near the excitation region of the parallel-plate mode, which is the gap region of the CBCPW, is superior to placing via holes randomly and shorting the periphery of the ground planes, which only causes a shift in the resonant frequencies of the ground planes. However, the use of metallic lateral walls and via holes increases the fabrication cost and contradicts one of the main advantages of the CPW technology that is no need of via holes for grounding.

The second method is to have the effective dielectric constant of the dominant CPW mode higher than that of the dominant parallel-plate TEM mode by introducing an additional dielectric layer, which has higher dielectric constant, either above or beneath the side planes [55]–[60], by use of finite-width dielectric-guide structure [42], [43], or by constructing a groove on the backside of CBCPW substrate [61], [62]. In [58], Liu et al. named the multilayered CBCPW's nonleaky coplanar (NLC) waveguides. Using NLC waveguides in the antenna applications can be found in [63]–[67]. Though the NLC waveguides themselves are no longer leaky, mode coupling between the dominant CPW mode and the dominant parallel-plate TEM mode occurs at discontinuities [30]. Due to the additional dielectric layer, the design of NLC waveguides become more complicated and leads to higher cost.

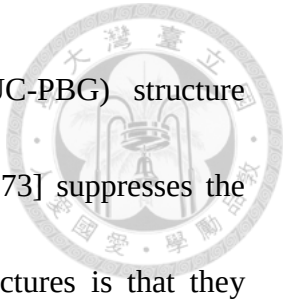

Third, using the uniplanar compact photonic bandgap (UC-PBG) structure [68]–[70] and the electromagnetic bandgap (EBG) structure [71]–[73] suppresses the parallel-plate mode leakage. The one common feature of the structures is that they exhibit a limited frequency band, called bandgap or stopband, where parallel plate modes are evanescent and hence, the parallel-plate mode leakage would be reduced effectively. The UC-PBG structure, realized with metal pads etched in the side ground planes connected by narrow lines to form a distributed *LC* network, is proved effective in reducing leakage of parallel-plate modes to the side ground planes of CBCPW [69], [70]. The other approaches applied to CBCPW are proposed to solve the leakage problems. They are leakage-reduced CBCPW with periodic structures [74], leakage suppressed CBCPW with patterned backside metallization [75], etched ground CBCPW [76], hollow CBCPW [77], and CBCPW using additional lossy substrate [78], [79].

For the applications requiring properties of satisfactory front radiation in the broadside direction and low back radiation, the patch antenna with electromagnetically coupled CPW feed-line has been proposed and widely investigated in the last two decades [80]–[91]. This structure usually consists of a patch antenna and feeding CPW, which are placed on the opposite sides of the substrate. The CPW-fed patch antenna couples the electromagnetic energy from the feed-line to the patch antenna through a coupling slot and thus, low back radiation is achieved with the aid of the ground plane

of CPW feed-line. There is another commonly used technique on reducing the back radiation from CPW-fed bi-directional antennas [92]–[97]. An additional conducting plane serving as a reflector is placed below the planar bi-directional antenna and parallel to the antenna surface. In addition, the optimum spacing between the bi-directional antenna and the reflector is nearly a quarter free-space wavelength. In that case, the radiation pattern with high front-to-back ratio is achieved. Although the input match of the antenna would be slightly altered, it can be compensated by a small alternation of the antenna size. The main drawback in this case is that the reflector must be placed about a quarter free-space wavelength away from the bi-directional antenna. The resulting structure is not of low profile nature at lower radio frequencies.

Sievenpiper et al. proposed high-impedance electromagnetic surfaces with a forbidden frequency band, which have high surface impedance. In addition, the surface reflects electromagnetic waves with no phase reversal, behaving as a kind of artificial magnetic conductor (AMC) [98]. Depending on the exhibited electromagnetic properties, the high-impedance electromagnetic surface has various names, such as EBG (electromagnetic bandgap) structure and AMC's [99]. AMC's have been successfully used as reflectors to render the radiation of CPW-fed antennas from bi-directional to uni-direction and the spacing between the CPW-fed antennas and AMC's are much smaller than that of conducting planes because AMC's have the property of 0° reflection

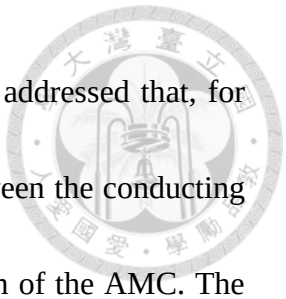

phase at specific frequency [73], [100]–[110]. In [106], it has been addressed that, for the slot antennas, the AMC performance of the whole structure between the conducting plane on which the slot is etched and the ground plane at the bottom of the AMC. The propagation of any modes between the two conducting planes (which effectively form the parallel plate cavity structure), and subsequent radiation from the edges of the structure should be minimized over the operating bandwidth [106].

Compared with the CPW-fed patch antennas and bi-directional antennas with reflectors, either conducting planes or AMC's, the CBCPW-fed antenna designs only use one substrate layer and when the BC is kept intact, back radiation of the CBCPW-fed antennas would be reduced naturally. Due to the simple structure and the ease of fabrication, the CBCPW-fed antenna designs are attractive in the applications that require the properties of low profile, reduced back radiation of antenna, and intact BC.

For the CBCPW-fed antenna design, some approaches have been developed. The first approach is the phase cancellation technique. Proposed in the 1980s, this technique deals with the surface wave problems of printed dipoles as well as slots on electrically thick substrate [111]–[116]. This technique utilizes twin broadside slots half a guided wavelength apart to cancel the unwanted propagating power. Lan et al. [117]–[120] and Lee et al. [121] used this technique to reduce the leakage of the parallel-plate mode and

to enhance the efficiency of the CBCPW-fed slot antenna. In [119], the antenna efficiency can be significantly improved from below 10% to 69.8%. Based on this antenna design, a modified design using two shorting strips can operate at the same frequency band with and without BC [122]. Good performance of the antenna design with and without BC is achieved. However, when the BC exists and finite ground plane used in the measurement, it can be observed from the measured input reflection coefficient that un-predicted resonances occur around the operating frequency. If the un-predicted resonances happen in the operating band, the antenna performance would be un-predictable. Thus, additional efforts are required to deal with the undesired resonances.

The second method is using side plane conductors to design CBCPW-fed side plane patch antennas [123], [124]. In [123], by etching a slotline pair on the side planes in the transverse direction of the CBCPW, the surface currents on the two side planes can be made the same phase and a broadside radiated patch antenna is obtained. In [124], two metallic strips placed a half guided-wavelength apart are used separately to connect the signal strip and the two side planes of the CBCPW. The side planes thus excited are resonating in phase and radiating in the broadside direction. These structures are simple and easy to design.

The final one is the CBCPW-fed coplanar patch antenna (CPA), which looks like a

CPW-inductively-fed slot loop antenna with BC [125]–[136]. The characteristics of CPA are similar to those of the conventional patch antenna. Although there are some differences between the two antennas, such as the geometric parameters and the parallel-plate mode leakage, the design rules for the conventional patch antenna can be used. The basic design considerations of CPA are straightforward.

1.3 CONTRIBUTION

This dissertation is devoted to the analysis and design of printed antenna fed by CPW with different backing materials.

In Chapter 2, hybrid designs of CPW-fed printed antenna with and without BC are presented. The hybrid designs can adapt themselves to the presence or absence of BC's. First, the original hybrid design is proposed, analyzed, and designed. When BC is placed, the antenna is a CBCPW-fed side plane patch antenna, while when BC is removed, the antenna becomes a CPW-fed slot dipole antenna. The antenna is designed to have the side plane patch and the slot dipole operate at the same frequency, so that it can adapt itself to the presence or absence of BC. In addition, miniaturization and bandwidth enhancement of the hybrid designs are presented, respectively. Compared with the original design, miniaturized design achieves roughly 40% reduction in size and the overlapping impedance bandwidth of the bandwidth-enhanced design is wider,

approximately three times of the original design.

In Chapter 3, design of an EBG-backed CPW-fed slot dipole antenna is presented. The antenna is formed by placing a CPW-fed slot dipole on the top of the EBG structure. It is found that the design considerations of the EBG-backed CPW-fed slot dipole are different from those of the conventional CPW-fed slot dipole. This is because the propagation characteristics of the EBG-backed slotline utilized in the EBG-backed design are quite different from those of the slotline for conventional design. By using the extracted propagation constant of the EBG-backed slotline, a detailed antenna design procedure is presented.

1.4 CHAPTER OUTLINES

This dissertation is organized in the sequence described below.

In Chapter 2, the hybrid designs of printed antenna fed by CPW with and without BC have three variants. First of all, an original hybrid design is proposed, designed, and fabricated. Design details and simulation and measurement results are also presented and discussed. Second, a compact hybrid design is proposed. The antenna design is demonstrated and simulation and measurement results are presented. Finally a bandwidth-enhanced hybrid design is proposed. Detailed antenna design is also presented. The antenna performance is verified by simulation and measurement results.

In Chapter 3, an EBG-backed CPW-fed slot dipole antenna is presented. Detailed antenna design procedure is presented. The propagation constant of the EBG-backed slotline is extracted and investigated first. Then, the proposed antenna is designed, fabricated, and tested. Simulation and measurement results are presented and discussed.

Finally, some conclusions are drawn in Chapter 4.

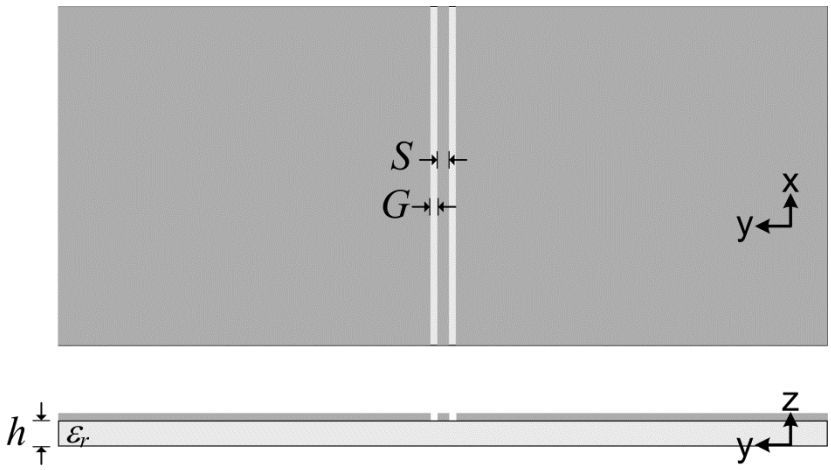

Fig. 1.1 Schematic of the coplanar waveguide (CPW).

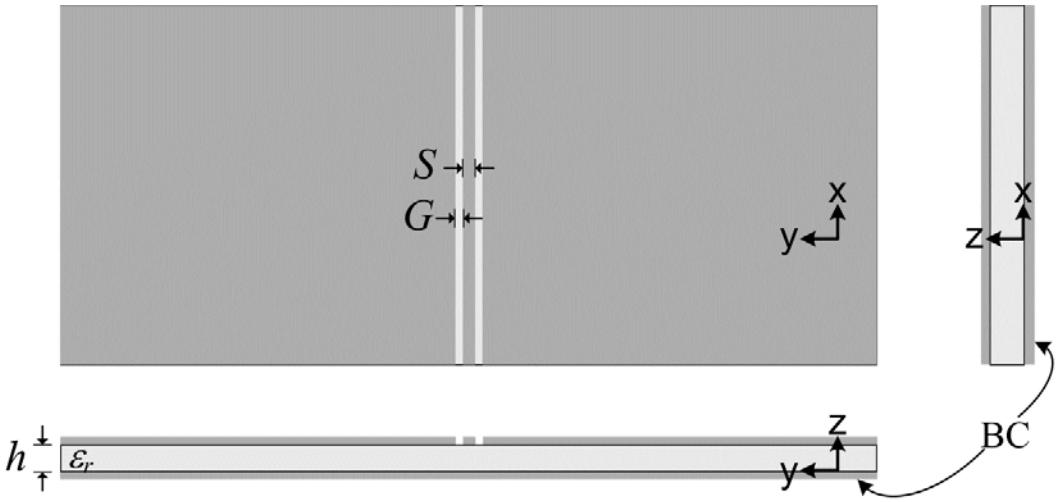

Fig. 1.2 Schematic of the conductor-backed CPW (CBCPW).

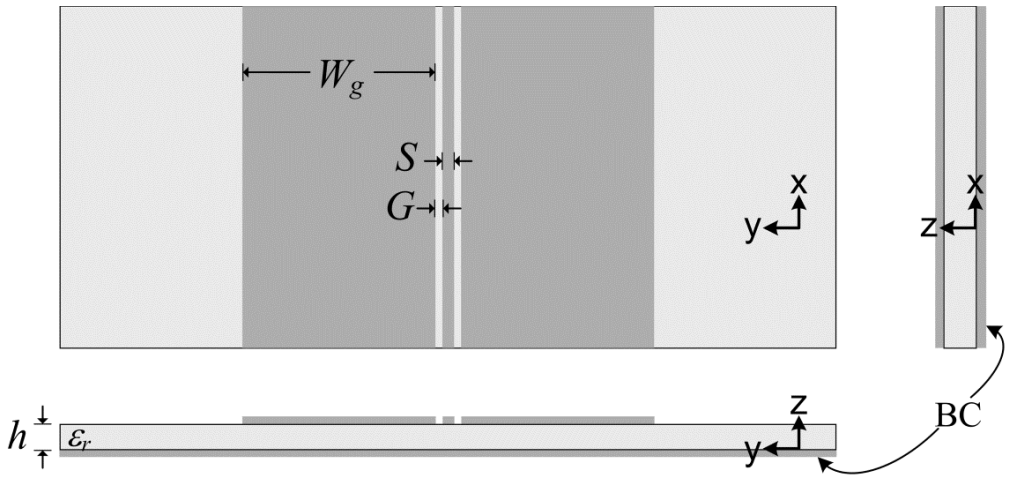

Fig. 1.3 Schematic of the finite-width CBCPW.

Chapter 2

Hybrid Designs of Printed Antenna Fed by Coplanar Waveguide With and Without Back Conductor

2.1 THE ORIGINAL CASE

A hybrid design of coplanar waveguide (CPW)-fed printed antenna with and without back conductor (BC) is presented. An E-shaped strip protruded from the signal strip of the feed line is used to connect the two side (ground) planes of the antenna. When BC is placed, the antenna is a conductor backed CPW (CBCPW)-fed side plane patch antenna, while when BC is removed, the antenna becomes a CPW-fed slot dipole antenna. The antenna is designed to have the side plane patch and the slot dipole operate at the same frequency, so that it can adapt itself to the presence or absence of BC. Resonant behaviors and radiation characteristics of the proposed hybrid antenna with and without BC are presented. Design details and simulation and measurement results are also presented and discussed.

2.1.1 Introduction

Coplanar waveguides (CPW's) as feed lines of printed antennas provide several advantages, such as low dispersion, easy implementation of shunt circuits, no need of via holes, and easy integration with monolithic microwave integrated circuits. To improve the mechanical strength of the substrate and the heat sink capability of the connected active circuits, a conducting sheet, called back conductor (BC), is usually placed at the back of the CPW [2]. This conductor-backed CPW (CBCPW) is known as an overmoded guided-wave structure [32]–[34], in which there exit a CPW mode and a microstrip-like (MSL) mode that have zero cutoff frequencies. When discontinuities in the CBCPW occur, energy would couple from the CPW mode to the MSL mode [32]–[34], which, in turn, would lead to the resonances of the side-plane conductors (ground planes of CPW). Then a large portion of the incident power would not be transmitted but rather be reflected and radiated. Hence the side-plane conductors could be used to design patch antennas and their resonant frequencies are predictable by employing the patch antenna theory [35], [36].

Using side-plane conductors to design CBCPW-fed patch antennas has been investigated [123], [124]. In [123], by etching a slotline pair on the side planes in the transverse direction of the CBCPW, the surface currents on the two side planes can be

made the same phase and a broadside radiated patch antenna is obtained with about 2% impedance bandwidth. In [124], two metallic strips placed a half guided-wavelength apart are used separately to connect the signal strip and the two side planes of the CBCPW. The side planes thus excited are resonating in phase and radiating in the broadside direction, and the measured impedance bandwidth is about 5.8%. The CBCPW-fed patch antennas [123], [124] are suitable for the wireless applications requiring BC's. However, when the BC's of the antennas are removed, their good antenna performance would be no longer maintained. They cannot be applied to the situations that BC's are removed.

In this section, a novel design of the CBCPW-fed side plane patch antenna is proposed. The two side planes of the proposed antenna are connected separately to the two side arms of an E-shaped strip protruded from the signal strip of the CBCPW. It will be shown that good impedance matching and broadside radiation of this CBCPW-fed side plane patch antenna are achieved. In addition to the good antenna performance, it is also observed that the E-shaped strip and the side planes form a slot dipole, which would radiate when the BC of CBCPW is removed. Then the proposed antenna becomes the conventional CPW-fed slot dipole, which is commonly used in many wireless applications. To have the proposed antenna operate both with and without the BC, the dimensions of the slot dipole are carefully adjusted so that it can resonate at the

same frequency as that of the originally proposed CBCPW-fed side plane patch antenna. Thus the proposed design becomes a hybrid design of antenna fed by the CPW with and without BC. Design details are presented, and simulation and measurement results are also presented and discussed.

2.1.2 Antenna Structure and Design

The geometry of the proposed hybrid antenna fed by the CPW with and without BC is shown in Fig. 2.1. The gray and light gray areas represent the metal part of the antenna and the substrate, respectively. There is a BC attached in Fig. 2.1(a), while no BC is attached in Fig. 2.1(b). The substrate and BC are designed to have the same size (same length L_{sub} and width W_{sub}), which is chosen a little larger than the antenna size for easy fabrication. The lower edges of the CPW feed-line and the substrate are aligned so that the CPW can be connected directly to a 50-Ω subminiature version A (SMA) connector.

In order to have the hybrid operation with and without BC, CBCPW and CPW feed-lines shown in Fig. 2.1(a) and (b), respectively, should have the same signal strip width S and the same gap width G. This, however, may lead to different effective dielectric constants (ε_{eff}'s) and different characteristic impedances (Z_0's) between them. Since CBCPW structure is a mixture of CPW and microstripline [25], to have the

characteristics of CBCPW tend to approach those of CPW, the electric coupling across the gaps of CBCPW should be as large as possible. Thus *G* should be chosen as small as possible, while *S* is determined to have Z_0's of CBCPW and CPW as close to 50 Ω as possible.

Consider the CBCPW-fed side plane patch antenna shown in Fig. 2.1(a) first. An E-shaped strip with dimensions *L*, *W*, and *T* protruded from the signal strip of the CBCPW is used to connect the two side plane conductors. Each side plane has dimensions of length L_1 and width W_1. L_1 is chosen approximately equal to half wavelength at the resonant frequency. The input match is then tuned by adjusting *L*, *W*, *T*, and W_1. It will be shown that the two side planes excited by the E-shaped strip and the MSL mode of the CBCPW will resonate in phase and radiate in the broadside direction.

When BC is removed from CBCPW, the MSL mode no longer exists, the side planes are now just the ground planes of CPW, and the antenna becomes a conventional slot dipole antenna fed inductively by a CPW, as shown in Fig. 2.1(b). To have the CPW-fed slot dipole resonate at the same frequency as that of the CBCPW-fed side plane patch, the dipole length *L* is chosen to be about one guided-wavelength at the resonant frequency. Then the input match of the antenna is tuned by adjusting the dipole width *W*. Combining all design considerations stated above, the proposed hybrid

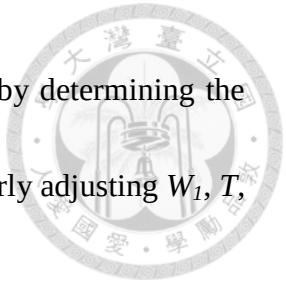

antenna fed by the CPW with and without BC should be designed by determining the resonant lengths L_1 and L first, then the input match is done by properly adjusting W_1, T, and W.

The substrate used in the designed is FR-4 with thickness h = 1.5 mm, dielectric constant ε_r = 4.2, and loss tangent $\tan\delta$ = 0.02. The operating frequency is chosen at 2.45 GHz. G is chosen to be 0.3 mm, which is the minimum gap width capable of in-house fabrication. S is determined to be 2 mm such that Z_0's of CBCPW and CPW are 45.3 and 53.8 Ω, respectively, and ε_{eff}'s are 2.67 and 2.35, respectively. For comparison, Z_0 and ε_{eff} of a 2-mm-wide microstripline with the same substrate are 62 Ω and 3.11, respectively. When G = 0.3 mm and S = 2 mm, the properties of the CBCPW are more similar to those of the CPW than those of the 2-mm-wide microstripline. All other parameters used are: L_1 = 28.87 mm, W_1 = 66.5 mm, L = 72.9 mm, L_{sub} = 44.97 mm, W_{sub} = 147.6 mm, W = 8.4 mm, and T = 1.7 mm. All simulations in the following are conducted by using ANSYS HFSS ver. 11.

2.1.3 Simulation and Measurement Results

Two CPW-fed printed antennas of the same geometric parameters listed above are fabricated. One is with and the other without BC. Fig. 2.2 shows the simulated and measured input reflection coefficients of the hybrid design. The discrepancies between

simulated and measured results may be due to the manufacturing tolerances. It can be seen that the antenna with and without BC have their resonant frequencies around 2.45 GHz, as predicted. The measured impedance bandwidths ($|S_{11}| \leq -10$ dB) of the antenna with and without BC are 3.2% (2.406–2.486 GHz) and 14.5% (2.294–2.655 GHz), respectively. The overlapping between them is 3.2% (2.406–2.486 GHz). This reveals that the proposed hybrid design can adapt itself to the presence or absence of BC with good impedance matching over a frequency band.

Parametric studies are conducted and plotted in Figs. 2.3 and 2.4. Fig. 2.3 shows the simulated input reflection coefficients with various L_1. All other parameters remain unchanged. The black lines in Fig. 2.3 show that the resonant frequency of the antenna with BC is indeed controlled by the length L_1. When the length increases, the resonant frequency decreases. The gray lines in Fig. 2.3 show that one resonant frequency is also observed when BC is absent, since in this case the side plane conductors are just the ground plane of CPW. Small perturbations on the ground planes by the different length of L_1 have almost no effect on the resonant behavior of the antenna without BC, so the resonant frequency is almost unchanged. Fig. 2.4 shows the simulated input reflection coefficients with various L while keeping other parameters unchanged. The black lines in Fig. 2.4 show that the variations in L have only a small effect on the impedance matching around the resonant frequency. This small impedance mismatch can be solved

by fine tuning W_1, T, and W. The gray lines in Fig. 2.4 show that the resonant frequency of the antenna without BC is decreased with increasing L. Figs. 2.3 and 2.4 conclude that the resonant frequencies of the antennas with and without BC are mainly controlled by the lengths L_1 and L, respectively. By carefully adjusting these resonant frequencies, together with fine tuning of W_1, T, and W, the overlapping impedance bandwidth between the antennas with and without BC can be maximized to cover a desired frequency band.

The instantaneous surface electric current distribution simulated at 2.45 GHz for the antenna with BC is plotted in Fig. 2.5. It is seen that the side plane conductors are strongly excited by the E-shaped strip and the MSL mode, thus they are the main radiators of the CBCPW-fed side plane patch antenna. When BC is absent, the antenna becomes a slot dipole antenna inductively fed by the CPW. The instantaneous magnetic current distribution simulated at 2.45 GHz for the slot dipole is shown in Fig. 2.6. It is seen that each arm of the slot dipole is nearly a half guided-wavelength long, and the total length of the slot dipole is about one guided-wavelength. Figs. 2.5 and 2.6 reveal that the antennas with and without BC have different resonant behaviors.

Simulated and measured gain patterns at 2.45 GHz for the antennas with and without BC are shown in Figs. 2.7 and 2.8, respectively. The measurements are carried out in an anechoic chamber and the antenna under test is fed by a coaxial cable from the

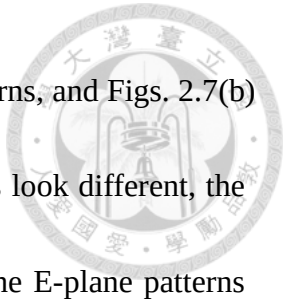

–x direction. Figs. 2.7(a) and 2.8(a) plot the E-plane (*x*-*z* plane) patterns, and Figs. 2.7(b) and 2.8(b) plot the H-plane (*y*-*z* plane) patterns. Though the patterns look different, the co-polarization components for the two antennas are the same. In the E-plane patterns shown in Figs. 2.7(a) and 2.8(a), the simulated E_ϕ components are invisible because they are smaller than the lower bound of the radial axis (–30 dBi). Ripples in the measured E_θ components may be attributed to the undesired radiation from the induced currents flowing onto the outer surface of the inevitable coaxial cable in the measurement [137]. The induced currents can be effectively suppressed by adding ferrite beads, a bazooka, or absorbers to the coaxial cable. We consider that some applications may use cables, so that the suppression methods are not used here to show the cable-related effects. From Fig. 2.7(a) and (b), it is seen that the main beam of the antenna with BC points in the broadside direction (+z or θ = 0° direction). The measured front-to-back (F/B) ratio is about 7 dB, which is small because the size of BC is just a little larger than the antenna on the top metal layer. The F/B ratio can be increased by enlarging the size of BC. When BC is absent, Fig. 2.8(a) and (b) show a dipole-like pattern, as expected. The measured F/B ratio is only about –0.4 dB, since the antenna without BC would radiate bi-directionally. The simulated and measured antenna gains and radiation efficiencies at 2.45 GHz are listed in Table I, where the measured radiation efficiencies are obtained by using the directivity/gain method described in

[138]. In this method, the directivity was obtained using the measured three-dimensional radiation pattern. The difference between simulated and measured antenna gains is ≤ 0.6 dB. The difference is also seen in the simulated and measured radiation efficiencies. This may also be caused by the coaxial cable used in the measurement. The simulated and measured radiation efficiencies of the antenna without BC are > 80%, while those of the antenna with BC are relatively low (< 50%). When the loss tangent of the substrate is reduced from 0.02 to 0.002, simulations show that the radiation efficiency for the antenna with BC can be improved from 42.8% to 85.6%. Thus, the radiation efficiency can be improved by using a low-loss substrate.

2.1.4 Summary

A hybrid design of CPW-fed printed antenna with and without BC has been presented. An E-shaped strip protruded from the signal strip of the feed line is used to feed the side plane conductors when BC is present, and the antenna is a CBCPW-fed side plane patch antenna. When BC is absent, the E-shaped strip and the side planes form a slot dipole, and the antenna becomes a CPW-fed slot dipole antenna. Both the patch antenna with BC and the slot dipole antenna without BC are designed to operate at the same frequency with the same geometric parameters. The measured overlapping impedance bandwidth between the two antennas is 3.2%. Resonant behaviors and

radiation characteristics of the hybrid antenna with and without BC have been shown to have satisfactory results and, indeed, it can adapt itself to the presence or absence of BC with good antenna performance.

2.2 THE COMPACT CASE

2.2.1 Introduction

A compact hybrid design of coplanar waveguide (CPW)-fed printed antenna with and without back conductor (BC) is presented. A Γ-shaped strip protruded from the signal strip of the feed line is used to connect one side (ground) plane of the antenna. When BC is placed, the antenna is a conductor backed CPW (CBCPW)-fed side plane patch antenna, while when BC is removed, the antenna becomes a CPW-fed half-wavelength slot. The antenna is designed to have the connected side plane patch and the half-wavelength slot operate at the same frequency, so that it can adapt itself to the presence or absence of BC. The side plane, which is not connected to the Γ-shaped strip, can be made small. When compared to the original design in the previous section, the compact design can achieve a 42% reduction in size at the cost of a smaller impedance bandwidth. Resonant behaviors and radiation characteristics of the compact hybrid antenna with and without BC are presented. Design details and simulation and measurement results are also presented and discussed.

2.2.2 Antenna Structure and Design

The geometry of the compact hybrid antenna fed by the CPW with and without BC

is shown in Fig. 2.9. The gray and light gray areas represent the metal part of the antenna and the substrate, respectively. There is a BC attached in Fig. 2.9(a), while no BC is attached in Fig. 2.9(b). The substrate and BC are designed to have the same size (same length L_{sub} and width W_{sub}), which is chosen a little larger than the antenna size for easy fabrication. The lower edges of the CPW feed-line and the substrate are aligned so that the CPW can be connected directly to a 50-Ω subminiature version A (SMA) connector.

First, the CBCPW-fed side plane patch antenna shown in Fig. 2.9(a) is considered. The CBCPW feed-line of length L_1 has side plane conductors of unequal widths. The right hand and left hand side plane conductors have widths W_1 and W_2, respectively. The width of the left hand side plane conductor (W_2) can be chosen small to reduce the occupied area of antenna, which will be shown later. A Γ-shaped strip with dimensions L, W, and T protruded from the signal strip of the CBCPW is used to connect the right hand side plane conductor (with length L_1 and width W_1). L_1 is chosen approximately equal to half wavelength at the resonant frequency. The input match is then tuned by adjusting L, W, T, and W_1.

When BC is removed from CBCPW, the MSL mode no longer exists, the side planes are now just the ground planes of CPW, and the antenna becomes a half-wavelength slot antenna fed by a CPW, as shown in Fig. 2.9(b). To have the

CPW-fed slot resonate at the same frequency as that of the CBCPW-fed side plane patch, the slot length L is chosen to be about a half guided-wavelength at the resonant frequency. Then the input match of the antenna is tuned by adjusting the slot width W. Combining all design considerations stated above, the proposed hybrid antenna fed by the CPW with and without BC should be designed by determining the resonant lengths L_1 and L first, then the input match is done by properly adjusting W_1, T, and W.

In order to have the hybrid operation with and without BC, CBCPW and CPW feed-lines shown in Fig. 2.9(a) and (b), respectively, should have the same signal strip width S and the same gap width G, the same right hand side plane conductor width W_1, and the same left hand side plane conductor width W_2. This, however, may lead to different effective dielectric constants (ε_{eff}'s) and different characteristic impedances (Z_0's) between them. Since CBCPW structure is a mixture of CPW and microstripline [25], to have the characteristics of CBCPW tend to approach those of CPW, the electric coupling across the gaps of CBCPW should be as large as possible. Thus G should be chosen as small as possible, while S is determined to have Z_0's of CBCPW and CPW as close to 50 Ω as possible. After determining G and S, it should be noted that, in the compact hybrid design, W_1 is usually large enough to have little effect on the Z_0's of CBCPW and CPW, while small W_2 may have large effect on the Z_0's. Thus, W_2 should be carefully chosen to achieve a compact design and have the Z_0's still close to 50 Ω.

The substrate used in the designed is FR-4 with thickness h = 1.5 mm, dielectric constant ε_r = 4.2, and loss tangent $\tan\delta$ = 0.02. The operating frequency is chosen at 2.45 GHz. The geometric parameters used are: G = 0.3 mm, S = 2 mm, L_1 = 28.9 mm, W_1 = 78.1 mm, W_2 = 5 mm, L = 40.8 mm, L_{sub} = 41.8 mm, W_{sub} = 97.7 mm, W = 5 mm, and T = 1.9 mm. Extracted by employing ANSYS Q3D Extractor, Z_0's of CBCPW and CPW are 44.9 and 53.3 Ω, respectively, both of which are close to 50 Ω, as desired. The antenna size of the original design in the section 2.1.2 and the compact design are 38.97 × 135.6 and 35.8 × 85.7 mm^2, respectively. The compact design can achieve a 42% reduction in size when compared to the original design. All simulations in the following are conducted by using ANSYS HFSS ver. 11.

2.2.3 Simulation and Measurement Results

Two CPW-fed printed antennas of the same geometric parameters listed above are fabricated. One is with and the other without BC. Fig. 2.10 shows the simulated and measured input reflection coefficients of the compact design. It can be seen that the antenna with and without BC have their resonant frequencies around 2.45 GHz, as predicted. The measured impedance bandwidths ($|S_{11}| \leq -10$ dB) of the antenna with and without BC are 2.5% (2.417–2.48 GHz) and 9.3% (2.346–2.577 GHz), respectively. The overlapping between them is 2.5% (2.417–2.48 GHz). This shows that the compact

hybrid design can adapt itself to the presence or absence of BC with good impedance matching over a frequency band.

Simulated and measured gain patterns at 2.45 GHz for the antennas with and without BC are shown in Figs. 2.11 and 2.12, respectively. The measurements are carried out in an anechoic chamber and the antenna under test is fed by a coaxial cable from the –x direction. Figs. 2.11(a) and 2.12(a) plot the E-plane (*x*-*z* plane) patterns, and Figs. 2.11(b) and 2.12(b) plot the H-plane (*y*-*z* plane) patterns. Though the patterns look different, the co-polarization components for the two antennas are the same. In the E-plane patterns shown in Figs. 2.11(a) and 2.12(a), ripples in the measured E_θ components may be attributed to the inevitable coaxial cable in the measurement [137]. From Fig. 2.11(a) and (b), it is seen that the main beam of the antenna with BC points in the broadside direction (+z or $\theta = 0°$ direction). When BC is absent, Fig. 2.12(a) and (b) show a bi-directional radiation pattern, as expected. The measured front-to-back (F/B) ratio is approximately 0 dB. The simulated and measured antenna gains and radiation efficiencies at 2.45 GHz for the antenna without BC are 3.85 and 3 dBi, respectively, and 91.2% and 75.1%, respectively, and those for the antenna with BC are 1.06 and 0.61 dBi, respectively, and 32.3% and 37.8%, respectively. It is observed that the radiation efficiencies for the antenna with BC in this section are a little lower than those of the original case in previous section. We have added air bridges to the CBCPW

transmission line to suppress the coupled slotline mode and the simulation shows that the radiation efficiency is almost the same, thus the reason may be that the MSL mode, which cannot be suppressed by the air brides, delivers some power to the left hand side plane, which radiates less. The difference between simulated and measured antenna gains is < 0.9 dB. The difference is also seen in the simulated and measured radiation efficiencies. This may also be caused by the coaxial cable used in the measurement. The simulated and measured radiation efficiencies of the antenna without BC are > 75%, while those of the antenna with BC are relatively low (< 40%). When the loss tangent of the substrate is reduced from 0.02 to 0.002, simulations show that the radiation efficiency for the antenna with BC can be improved from 32.3% to 76.4%. Thus, the radiation efficiency can be improved by using a low-loss substrate.

2.2.4 Summary

A compact hybrid design of CPW-fed printed antenna with and without BC has been presented. A Γ-shaped strip protruded from the signal strip of the feed line is used to feed the right hand side of the plane conductor when BC is present, and the antenna is a CBCPW-fed side plane patch antenna. When BC is absent, the Γ-shaped strip and the right hand side plane form a half-wavelength slot, and the antenna becomes a CPW-fed half-wavelength slot antenna. Both the patch antenna with BC and the half-wavelength

slot antenna without BC are designed to operate at the same frequency with the same geometric parameters. The measured overlapping impedance bandwidth between the two antennas is 2.5%. Resonant behaviors and radiation characteristics of the compact hybrid antenna with and without BC have been shown to have satisfactory results and, indeed, it can adapt itself to the presence or absence of BC with good antenna performance. Also, compared with the original design in the previous section, the compact design can achieve a 42% reduction in size.

2.3 THE BANDWIDTH-ENHANCED CASE

A bandwidth-enhanced hybrid design of coplanar waveguide (CPW)-fed printed antenna with and without back conductor (BC) is presented. An E-shaped strip protruded from the signal strip of the feed line is used to connect the two side (ground) planes of the antenna, and a pair of thin slits cut in the side planes adjacent to the two side arms of the E-shaped strip is employed to tune the input impedance of the antenna with BC. When BC is placed, the antenna is a bandwidth-enhanced conductor backed CPW (CBCPW)-fed side plane patch antenna, while when BC is removed, the antenna becomes a CPW-fed slot dipole antenna. The antenna is designed to have the side plane patch and the slot dipole operate at the same frequency, so that it can adapt itself to the presence or absence of BC. Resonant behaviors and radiation characteristics of the proposed hybrid antenna with and without BC are presented. Design details and simulation and measurement results are also presented and discussed.

2.3.1 Introduction

In this section, a novel design of the CBCPW-fed side plane patch antenna is proposed to further increase the impedance bandwidth. The two side planes of the proposed antenna are connected separately to the two side arms of an E-shaped strip protruded from the signal strip of the CBCPW. A pair of thin slits cut in the side planes

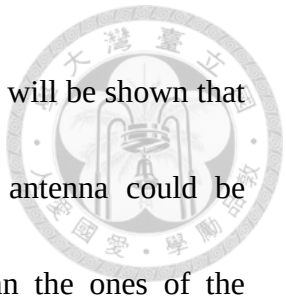

adjacent to the two side arms is used to tune the input impedances. It will be shown that the impedance bandwidth of this CBCPW-fed side plane patch antenna could be increased to about 9.9%, which is roughly three times wider than the ones of the original and compact designs with BC's in the previous sections. In addition to the increase in bandwidth, the E-shaped strip and the side planes form a slot dipole, which would radiate when the BC of CBCPW is removed. Then the proposed antenna becomes the conventional CPW-fed slot dipole. To have the proposed antenna operate both with and without the BC, the dimensions of the slot dipole are carefully adjusted so that it can resonate at the same frequency as that of the originally bandwidth-enhanced CBCPW-fed side plane patch antenna. Thus the proposed design becomes a hybrid design of antenna fed by the CPW with and without BC. Design details are presented, and simulation and measurement results are also presented and discussed.

2.3.2 Antenna Structure and Design

The geometry of the bandwidth-enhanced hybrid antenna fed by the CPW with and without BC is shown in Fig. 2.13. The gray and light gray areas represent the metal part of the antenna and the substrate, respectively. There is a BC attached in Fig. 2.13(a), while no BC is attached in Fig. 2.13(b). The substrate and BC are designed to have the same size (same length L_{sub} and width W_{sub}), which is chosen a little larger than the

antenna size for easy fabrication. The lower edges of the CPW feed-line and the substrate are aligned so that the CPW can be connected directly to a 50-Ω SMA connector.

In order to have the hybrid operation with and without BC, CBCPW and CPW feed-lines shown in Fig. 2.13(a) and (b), respectively, should have the same signal strip width S and the same gap width G. This, however, may lead to different effective dielectric constants (ε_{eff}'s) and different characteristic impedances (Z_0's) between them. Since CBCPW structure is a mixture of CPW and microstripline [25], to have the characteristics of CBCPW tend to approach those of CPW, the electric coupling across the gaps of CBCPW should be as large as possible. Thus G should be chosen as small as possible, while S is determined to have Z_0's of CBCPW and CPW as close to 50 Ω as possible.

Consider the CBCPW-fed side plane patch antenna shown in Fig. 2.13(a) first. An E-shaped strip with dimensions L, W, and T protruded from the signal strip of the CBCPW is used to connect the two side plane conductors. A pair of thin slits with length L_e and width W_e is cut in the side planes adjacent to the two side arms of the E-shaped strip. Each side plane is divided by the thin slit into two parts with lengths L_1, L_2, and L_3, which are chosen approximately equal to half wavelengths at three different but close resonant frequencies. By adjusting these three resonant frequencies, the

impedance bandwidth of the antenna can be suitably enlarged. The input match is then tuned by adjusting L, W, T, L_e and W_e. It will be shown that the two side planes excited by the E-shaped strip and the MSL mode of the CBCPW will resonate in phase and radiate in the broadside direction.

When BC is removed from CBCPW, the MSL mode no longer exists, the side planes are now just the ground planes of CPW, and the antenna becomes a conventional slot dipole antenna fed inductively by a CPW, as shown in Fig. 2.13(b). Although the relatively short thin slits in the x-direction have a little effect on the antenna performance, they have almost no effect on the resonant behavior of the slot dipole in the y-direction. To have the CPW-fed slot dipole resonate at the same frequency as that of the CBCPW-fed side plane patch, the dipole length L is chosen to be about one guided-wavelength at the resonant frequency. Then the input match of the antenna is tuned by adjusting the dipole width W. Combining all design considerations stated above, the proposed hybrid antenna fed by the CPW with and without BC should be designed by determining the resonant lengths L_1, L_2, L_3, and L first, then the input match is done by properly adjusting L_e, W_e, T, and W.

The substrate used in the designed is FR-4 with thickness h = 1.5 mm, dielectric constant ε_r = 4.2, and loss tangent $\tan\delta$ = 0.02. The operating frequency is chosen at 2.45 GHz, which is the center frequency of 2.4-GHz band (2.4–2.5 GHz) for industrial,

scientific, and medical (ISM) applications. G is chosen to be 0.3 mm, which is the minimum gap width capable of in-house fabrication. S is determined to be 2 mm such that Z_0's of CBCPW and CPW are 45.3 and 53.8 Ω, respectively. All other parameters used are: L_1 = 29.5 mm, L_2 = 28.3 mm, L_3 = 29.15 mm, L = 75.1 mm, W = 6.9 mm, L_e = 11 mm, W_e = 0.5 mm, L_{sub} = 44.1 mm, W_{sub} = 149.8 mm, and T = 1.7 mm. All simulations in the following are conducted by using ANSYS HFSS ver. 11.

2.3.3 Simulation and Measurement Results

Two CPW-fed printed antennas of the same geometric parameters listed above are fabricated. One is with and the other without BC. Fig. 2.14 shows the simulated and measured input reflection coefficients of the hybrid design. The discrepancies between simulated and measured results may be due to the manufacturing tolerances. It can be seen that the antenna with and without BC have three and one resonant frequencies, respectively, as predicted. The measured impedance bandwidths ($|S_{11}| \leq -10$ dB) of the antenna with and without BC are 9.9% (2.395–2.646 GHz) and 14% (2.337–2.69 GHz), respectively. The overlapping between them is 9.9% (2.395–2.646 GHz), which can cover the entire 2.4-GHz ISM band (2.4–2.5 GHz). This reveals that the proposed hybrid design can adapt itself to the presence or absence of BC with good impedance matching over a frequency band for wireless applications.

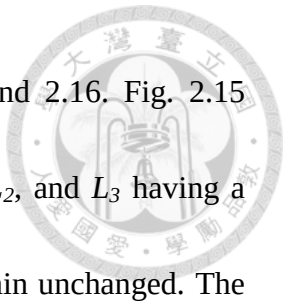

Parametric studies are conducted and plotted in Figs. 2.15 and 2.16. Fig. 2.15 shows the simulated input reflection coefficients with various L_1, L_2, and L_3 having a fixed ratio of 1:0.959:0.988 among them. All other parameters remain unchanged. The black lines in Fig. 2.15 show that the resonant frequencies of the antenna with BC are indeed controlled by the lengths L_1, L_2, and L_3. When these lengths increase simultaneously, the three resonant frequencies decrease simultaneously. The gray lines in Fig. 2.15 show that only one resonant frequency is observed when BC is absent, since in this case the side plane conductors are just the ground plane of CPW. Small perturbations on the ground planes by the different lengths of L_1, L_2, and L_3 have almost no effect on the resonant behavior of the antenna without BC, so the resonant frequency is almost unchanged. Fig. 2.16 shows the simulated input reflection coefficients with various L while keeping other parameters unchanged. The black lines in Fig. 2.16 show that the lower and upper resonant frequencies of the antenna with BC remain almost unchanged. The variations in L have only a small effect on the impedance matching around the middle resonant frequency. This small impedance mismatch can be solved by fine tuning L_e, W_e, T, and W. The gray lines in Fig. 2.16 show that the resonant frequency of the antenna without BC is decreased with increasing L. Figs. 2.15 and 2.16 conclude that the resonant frequencies of the antennas with and without BC are mainly controlled by the dimensions of the side-plane conductors (L_1, L_2, and L_3) and the length

L, respectively. By carefully adjusting these resonant frequencies, together with fine tuning of L_e, W_e, T, and W, the overlapping impedance bandwidth between the antennas with and without BC can be maximized.

The instantaneous surface electric current distribution simulated at 2.45 GHz for the antenna with BC is plotted Fig. 2.17. It is seen that the side plane conductors are strongly excited by the E-shaped strip and the MSL mode, thus they are the main radiators of the CBCPW-fed side plane patch antenna. When BC is absent, the antenna becomes a slot dipole antenna inductively fed by the CPW. The instantaneous magnetic current distribution simulated at 2.45 GHz for the slot dipole is shown in Fig. 2.18. It is seen that each arm of the slot dipole is nearly a half guided-wavelength long, and the total length of the slot dipole is about one guided-wavelength. Figs. 2.17 and 2.18 reveal that the antennas with and without BC have different resonant behaviors.

Simulated radiation patterns at the three resonant frequencies (2.45, 2.55, and 2.65 GHz) for the antenna with BC are plotted in Fig. 2.19. The co-polarization components at the three resonant frequencies are the same. In the E-plane pattern shown in Fig. 2.19(a), the simulated E_ϕ components are invisible because they are smaller than the lower bound of the radial axis (–30 dB). Simulated and measured gain patterns at 2.45 GHz for the antennas with and without BC are shown in Figs. 2.20 and 2.21, respectively. The measurements are carried out in an anechoic chamber and the antenna

under test is fed by a coaxial cable from the –x direction. Figs. 2.20(a) and 2.21(a) plot the E-plane (*x*-*z* plane) patterns, and Figs. 2.20(b) and 2.21(b) plot the H-plane (*y*-*z* plane) patterns. Though the patterns look different, the co-polarization components for the two antennas are the same. In the E-plane patterns shown in Figs. 2.20(a) and 2.21(a), the simulated E_ϕ components are invisible because they are smaller than the lower bound of the radial axis (–30 dBi). Ripples in the measured E_θ components may be attributed to the inevitable coaxial cable in the measurement [137]. From Fig. 2.20(a) and (b), it is seen that the main beam of the antenna with BC points in the broadside direction (+z or $\theta = 0°$ direction). The measured front-to-back (F/B) ratio is about 7 dB, which is small because the size of BC is just a little larger than the antenna on the top metal layer. The F/B ratio can be increased by enlarging the size of BC. When BC is absent, Fig. 2.21(a) and (b) show a dipole-like pattern, as expected. The measured F/B ratio is only about –0.4 dB, since the antenna without BC would radiate bi-directionally. The measured gains of the antennas with and without BC are in the range of 1.76–5.22 dBi over the overlapping frequency band (2.395–2.646 GHz) between the two antennas. The simulated and measured antenna gains and radiation efficiencies at 2.45 GHz are listed in Table II. The difference between simulated and measured antenna gains is ≤ 0.5 dB. The difference is also seen in the simulated and measured radiation efficiencies. This may also be caused by the coaxial cable used in the measurement. The simulated

and measured radiation efficiencies of the antenna without BC are > 80%, while those of the antenna with BC are relatively low (< 50%). When the loss tangent of the substrate is reduced from 0.02 to 0.002, simulations show that the radiation efficiency for the antenna with BC can be improved from 42.5% to 84.8%. Thus, the radiation efficiency can be improved by using a low-loss substrate.

2.3.4 Summary

A bandwidth-enhanced hybrid design of CPW-fed printed antenna with and without BC has been presented. An E-shaped strip protruded from the signal strip of the feed line is used to feed the side plane conductors when BC is present, and the antenna is a bandwidth-enhanced CBCPW-fed side plane patch antenna. When BC is absent, the E-shaped strip and the side planes form a slot dipole, and the antenna becomes a CPW-fed slot dipole antenna. Both the patch antenna with BC and the slot dipole antenna without BC are designed to operate at the same frequency with the same geometric parameters. The measured overlapping impedance bandwidth between the two antennas is 9.9% (2.395–2.646 GHz), which is wide enough to cover the entire ISM band (2.4–2.5 GHz) for wireless communications. Also, the overlapping is roughly three times wider than the ones of the original and compact designs in the previous sections. Resonant behaviors and radiation characteristics of the hybrid antenna with and without

BC have been shown to have satisfactory results and, indeed, it can adapt itself to the presence or absence of BC with good antenna performance. Thus whether or not the BC is used or not can depend upon the system requirements, which is very attractive in the wireless applications.

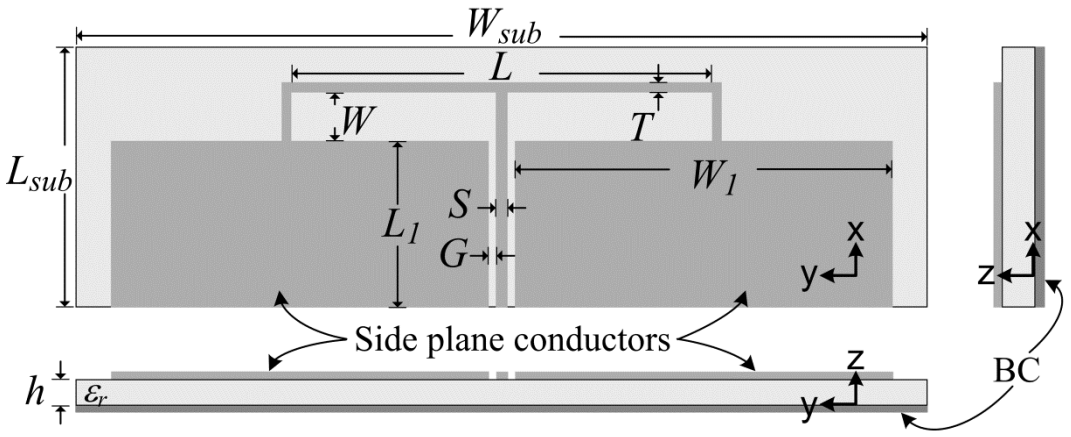

(a)

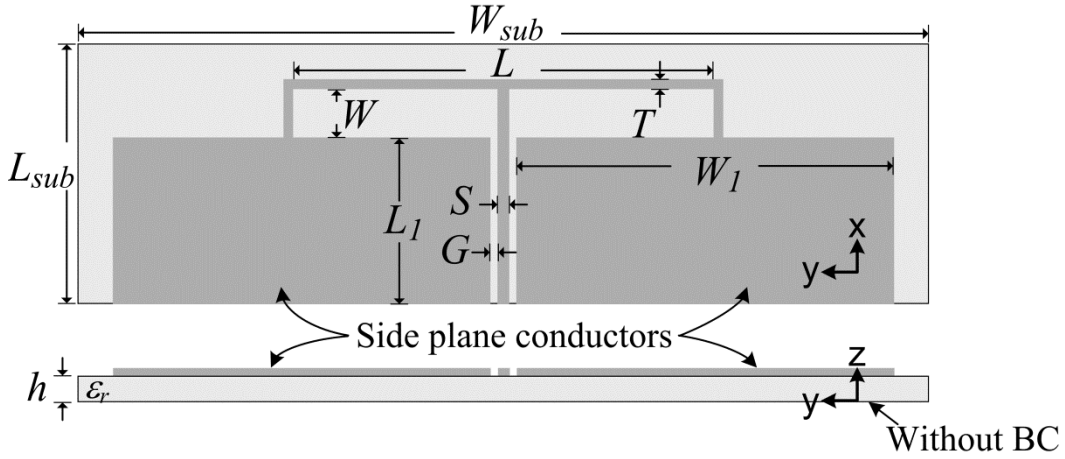

(b)

Fig. 2.1 Geometry of the proposed hybrid antenna fed by the CPW with and without BC.

(a) With BC and (b) without BC.

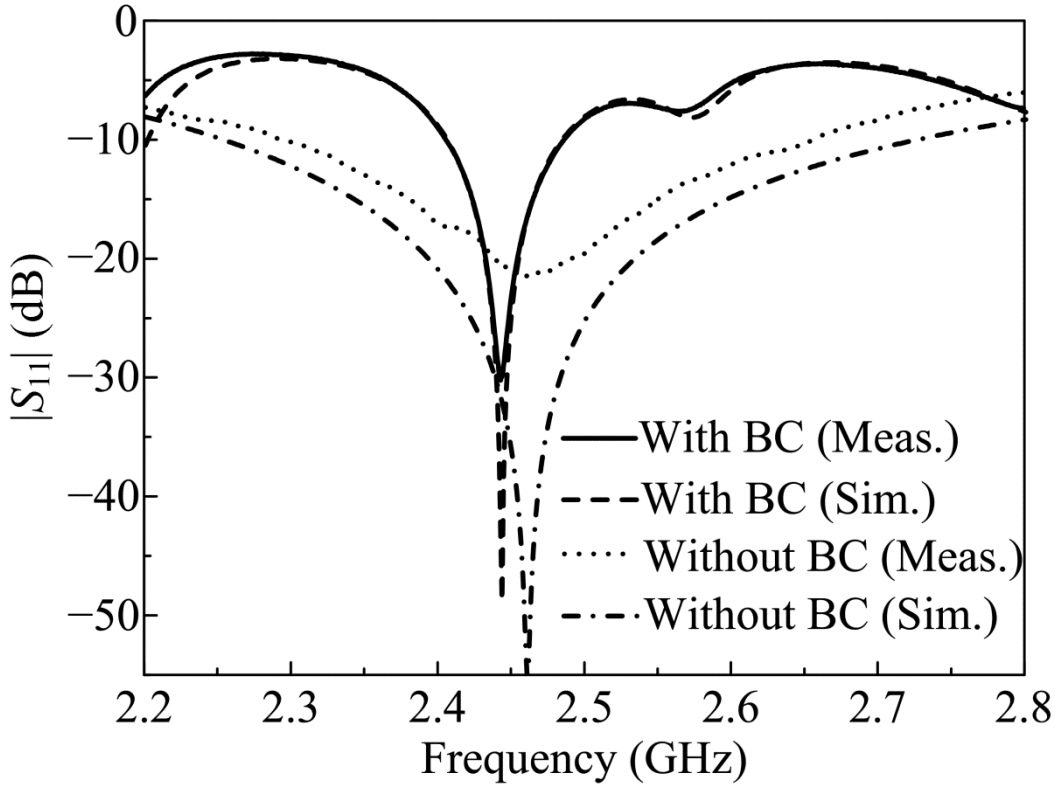

Fig. 2.2 Simulated and measured input reflection coefficients of the proposed hybrid antenna. Sim: simulation; Meas: measurement.

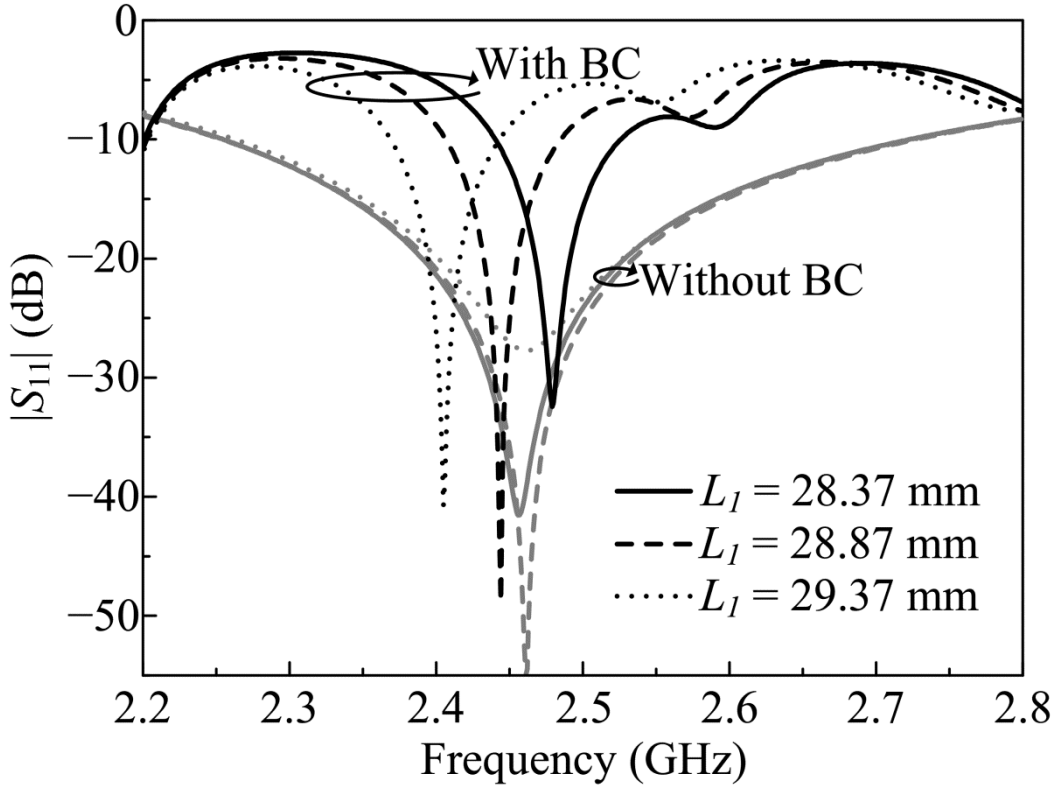

Fig. 2.3 Simulated input reflection coefficients with various L_1. Black line: with BC. Gray line: without BC.

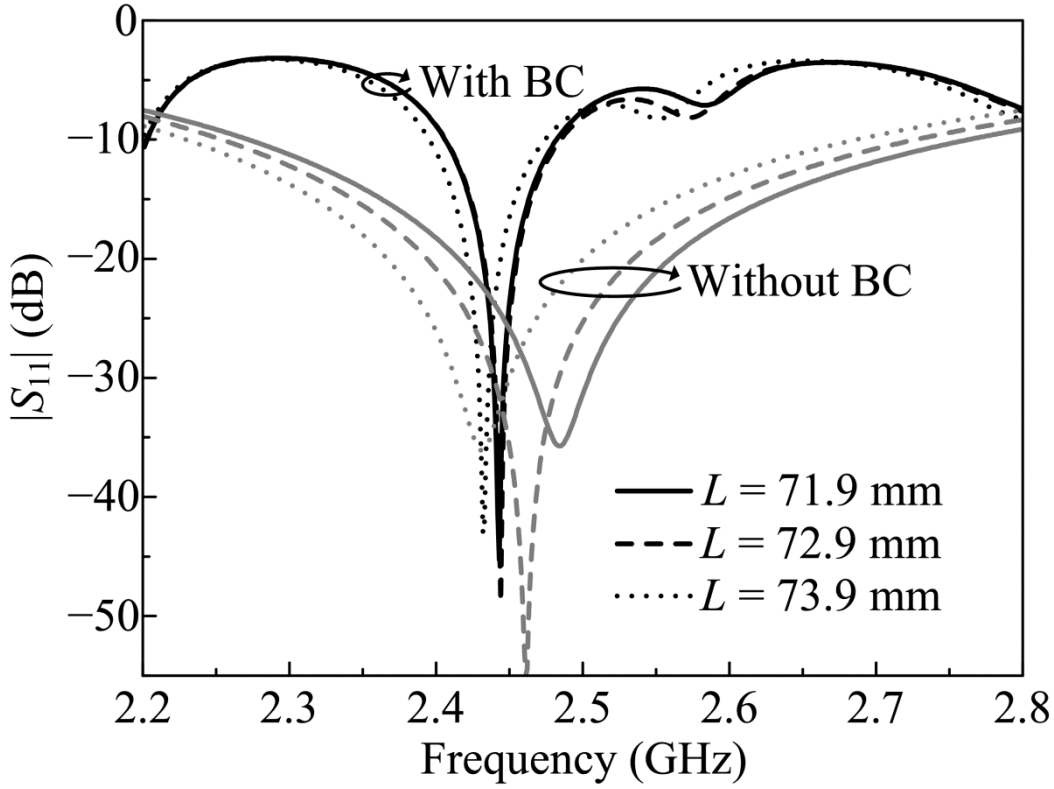

Fig. 2.4 Simulated input reflection coefficients with various *L*. Black line: with BC. Gray line: without BC.

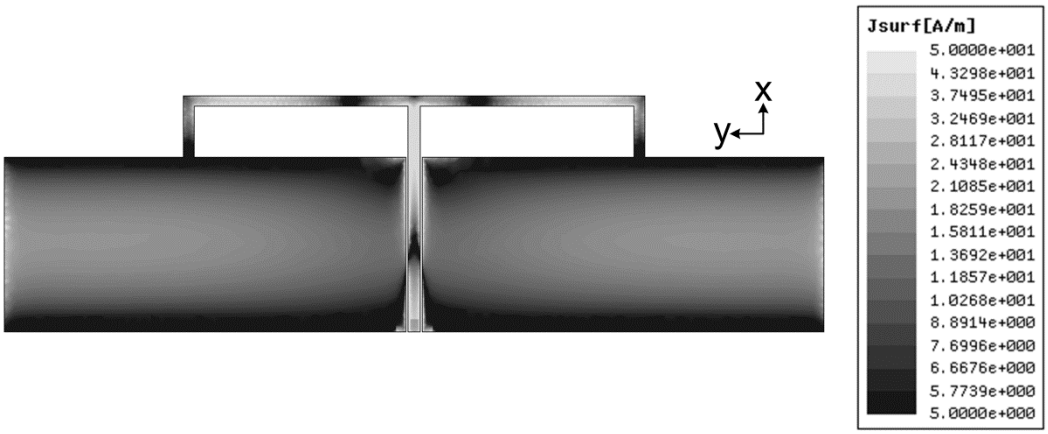

Fig. 2.5 Simulated surface electric current distribution for the antenna with BC at 2.45 GHz.

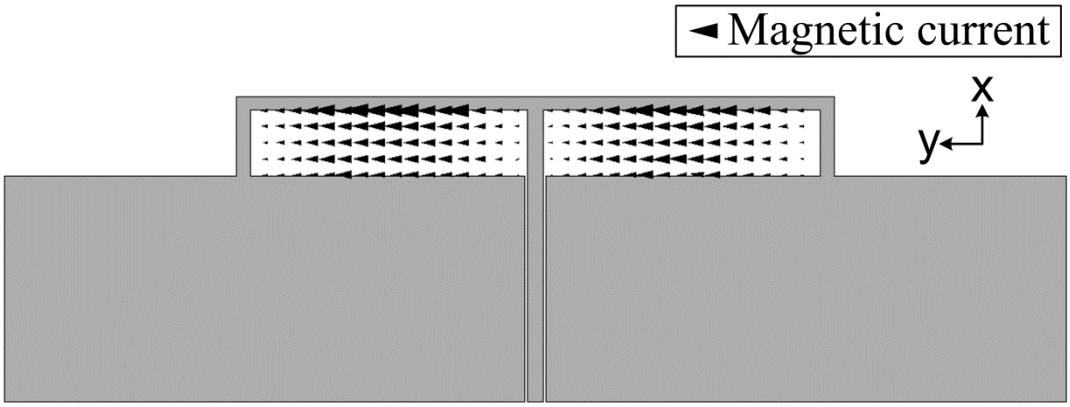

Fig. 2.6 Simulated equivalent magnetic current distribution in the slot dipole of the antenna without BC at 2.45 GHz.

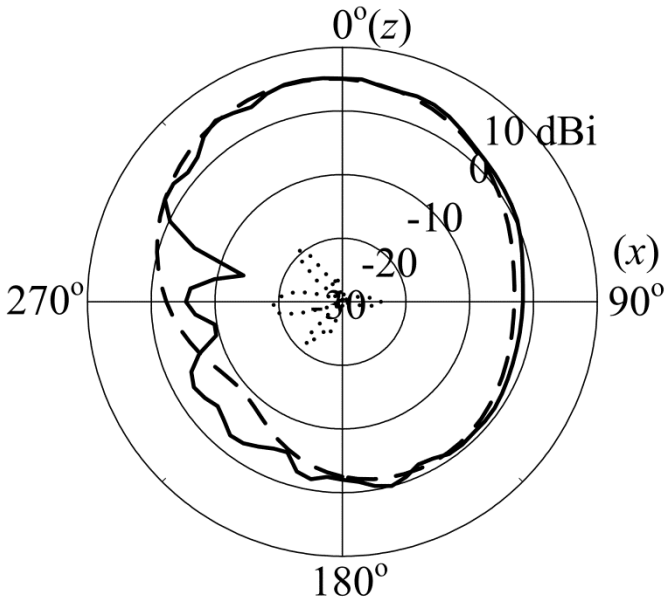

(a)

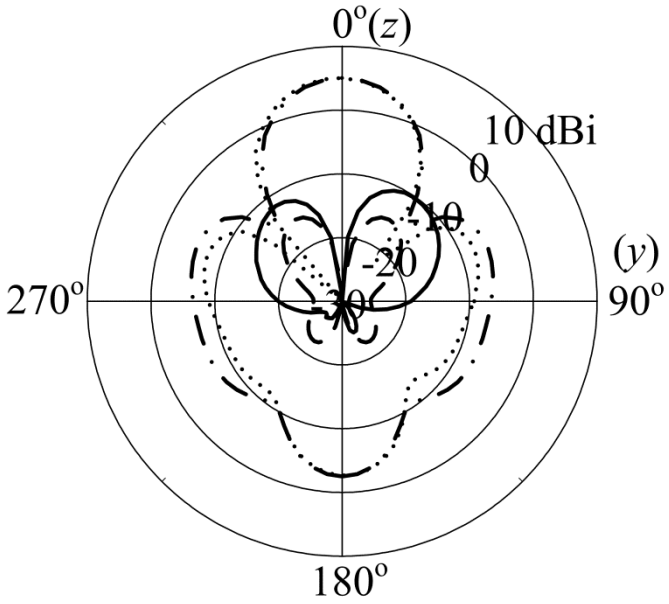

(b)

Fig. 2.7 Gain patterns of the antenna with BC at 2.45 GHz. (a) E-plane (*x*-*z* plane) and (b) H-plane (*y*-*z* plane). Solid line: measured E_θ. Dashed line: simulated E_θ. Dotted line: measured E_ϕ. Dash-dotted line: simulated E_ϕ.

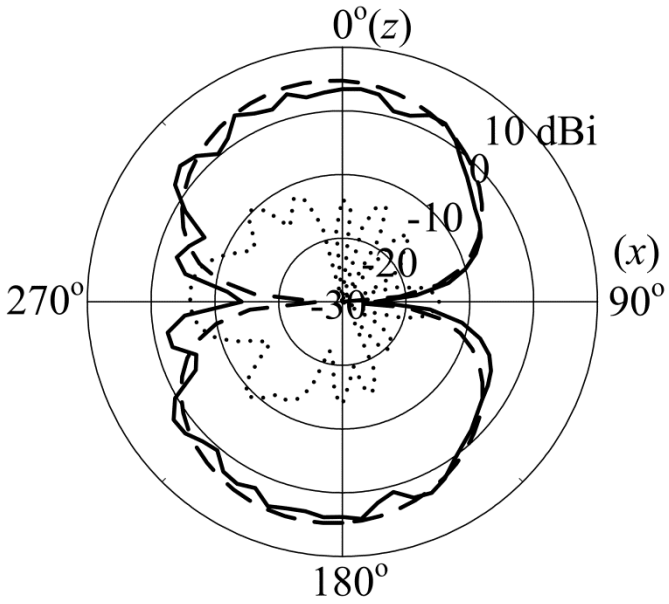

(a)

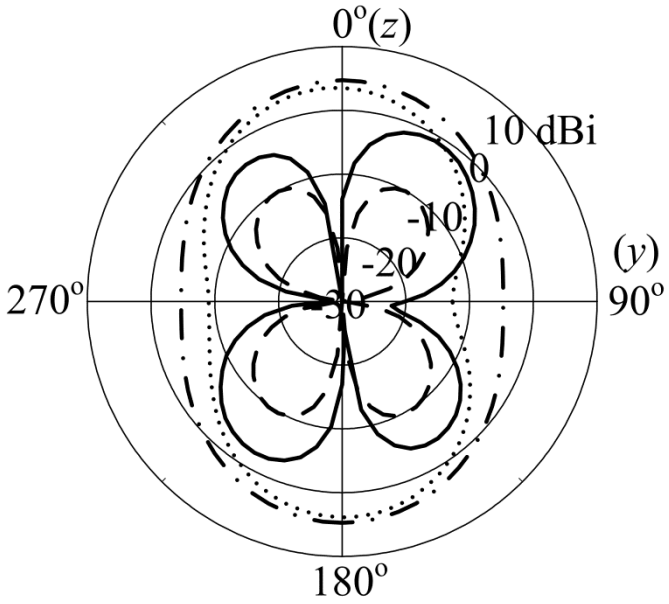

(b)

Fig. 2.8 Gain patterns of the antenna without BC at 2.45 GHz. (a) E-plane (*x*-*z* plane) and (b) H-plane (*y*-*z* plane). Solid line: measured E_θ. Dashed line: simulated E_θ. Dotted line: measured E_ϕ. Dash-dotted line: simulated E_ϕ.

TABLE I

SIMULATED AND MEASURED ANTENNA GAINS AND RADIATION EFFICIENCIES AT 2.45 GHZ

	Without BC		With BC	
	Sim.	Meas.	Sim.	Meas.
Antenna gain (dBi)	4.8	4.6	5.1	5.7
Radiation efficiency (%)	91.2	86.1	42.8	47.7

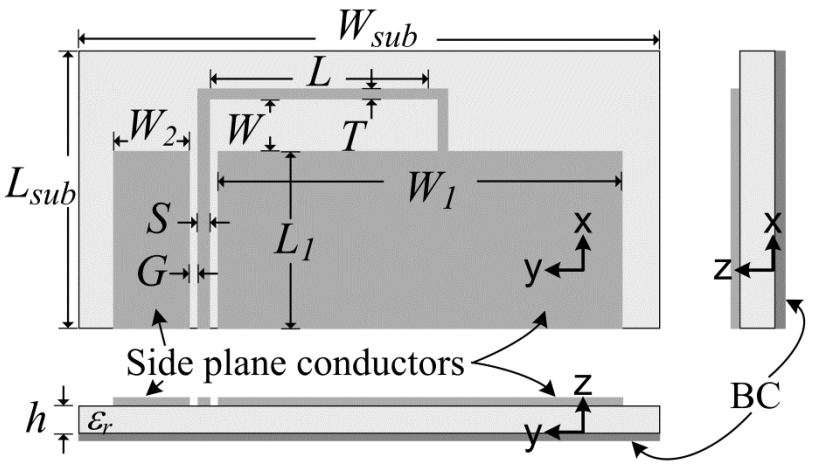

(a)

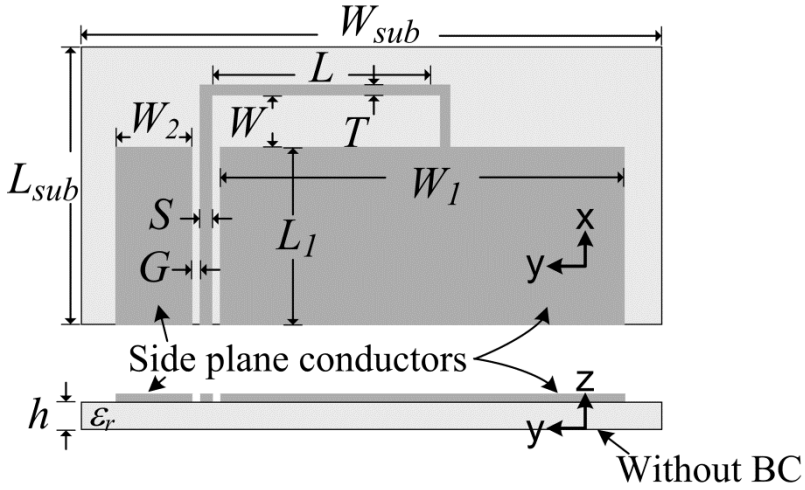

(b)

Fig. 2.9 Geometry of the compact hybrid antenna fed by the CPW with and without BC.

(a) With BC and (b) without BC.

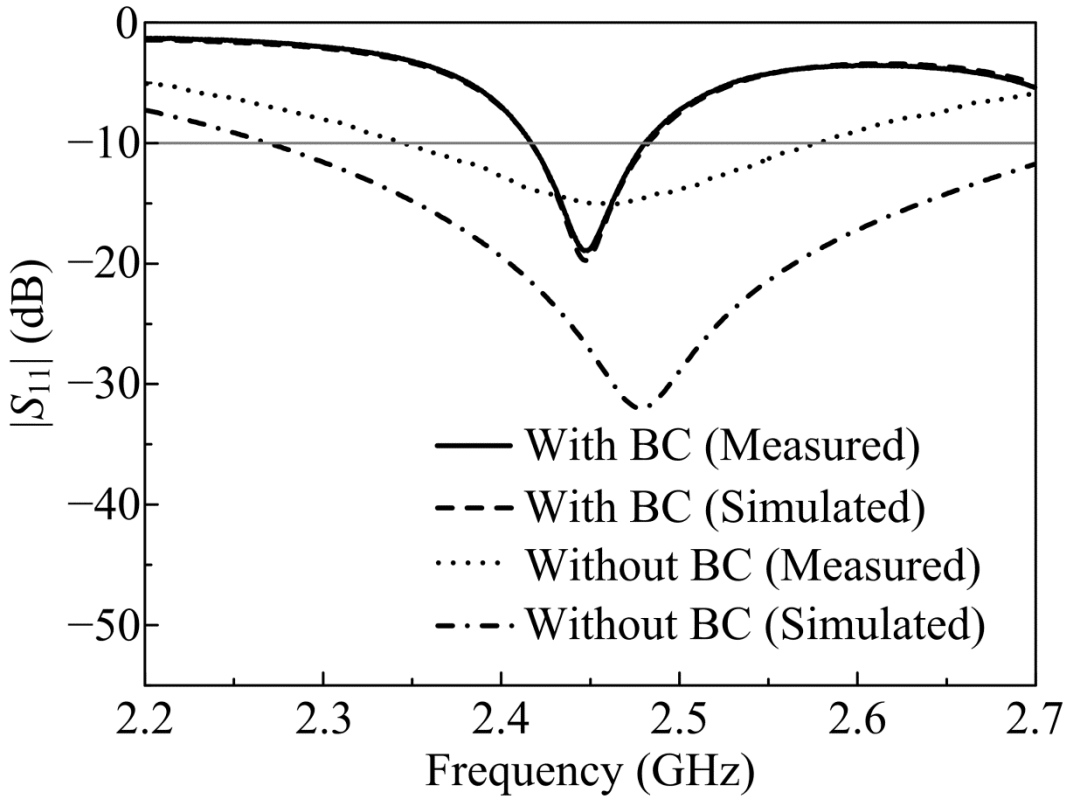

Fig. 2.10 Simulated and measured input reflection coefficients of the compact hybrid antenna.

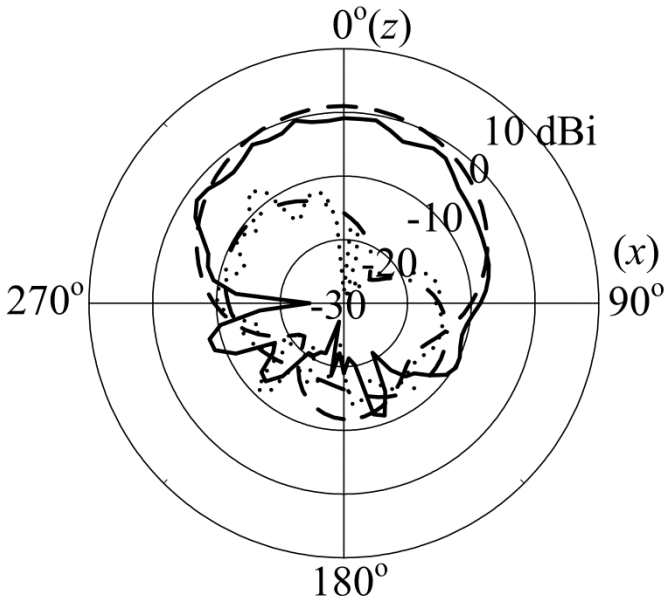

(a)

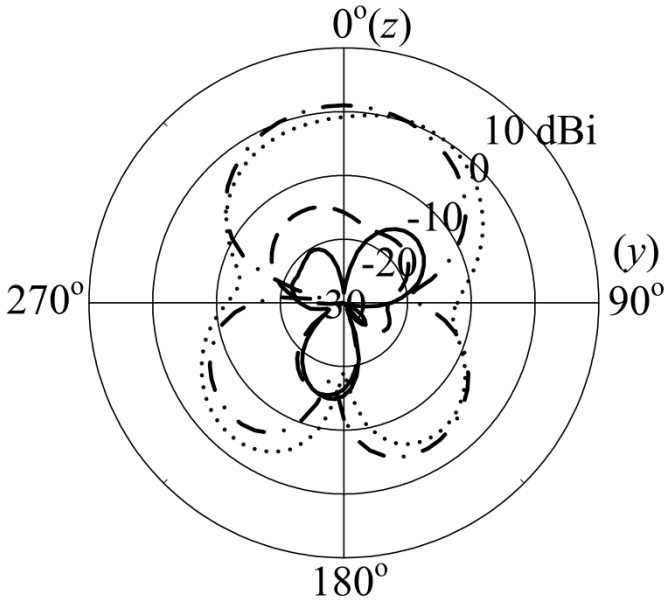

(b)

Fig. 2.11 Gain patterns of the compact antenna with BC at 2.45 GHz. (a) E-plane (*x*-*z* plane) and (b) H-plane (*y*-*z* plane). Solid line: measured E_θ. Dashed line: simulated E_θ. Dotted line: measured E_ϕ. Dash-dotted line: simulated E_ϕ.

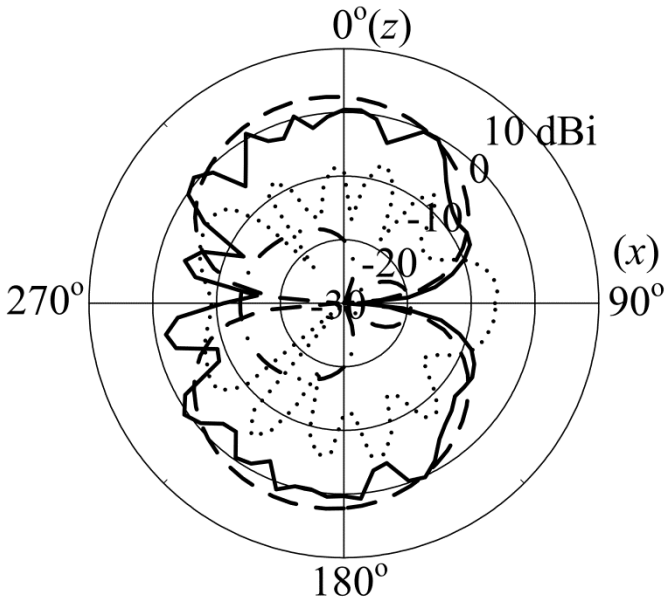

(a)

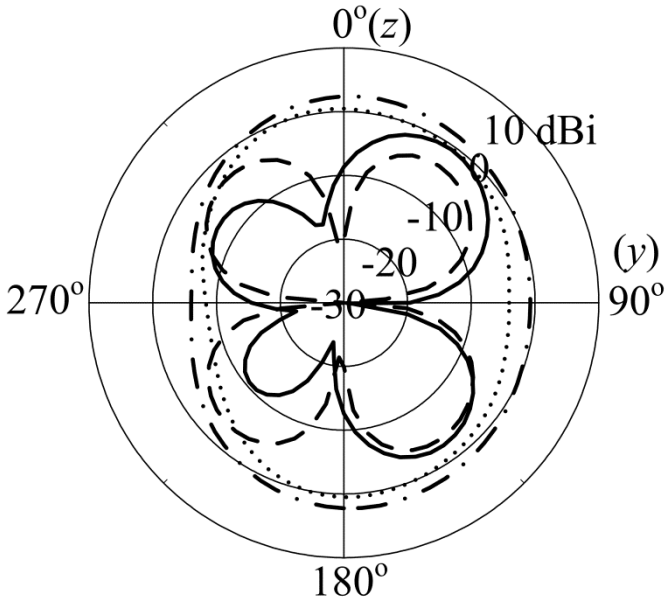

(b)

Fig. 2.12 Gain patterns of the compact antenna without BC at 2.45 GHz. (a) E-plane (*x*-*z* plane) and (b) H-plane (*y*-*z* plane). Solid line: measured E_θ. Dashed line: simulated E_θ. Dotted line: measured E_ϕ. Dash-dotted line: simulated E_ϕ.

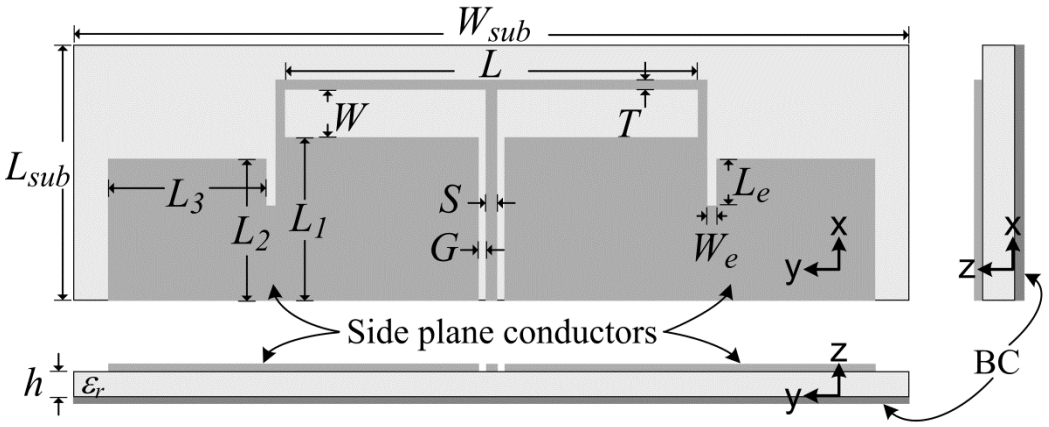

(a)

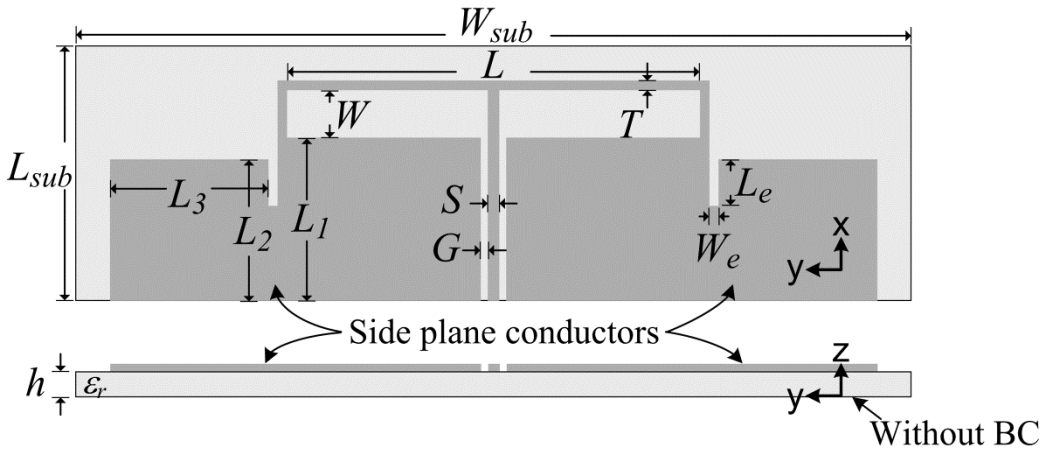

(b)

Fig. 2.13 Geometry of the bandwidth-enhanced hybrid antenna fed by the CPW with and without BC. (a) With BC and (b) without BC.

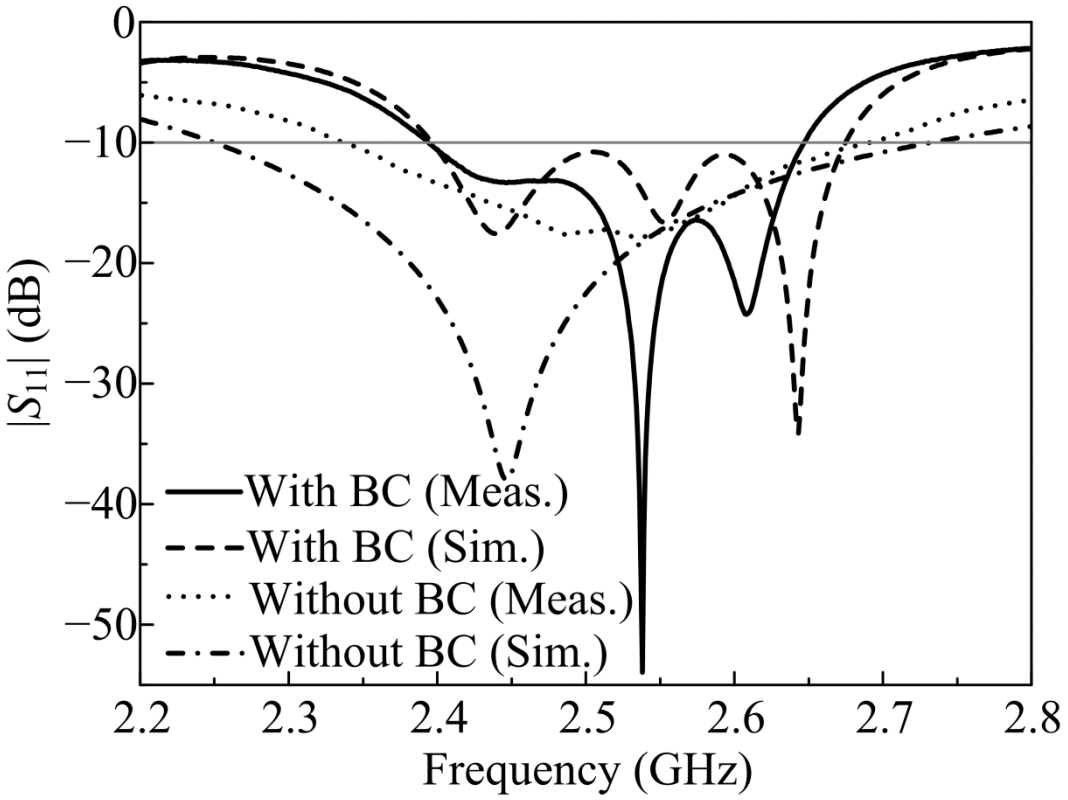

Fig. 2.14 Simulated and measured input reflection coefficients of the hybrid antenna with bandwidth enhancement. Sim: simulation; Meas: measurement.

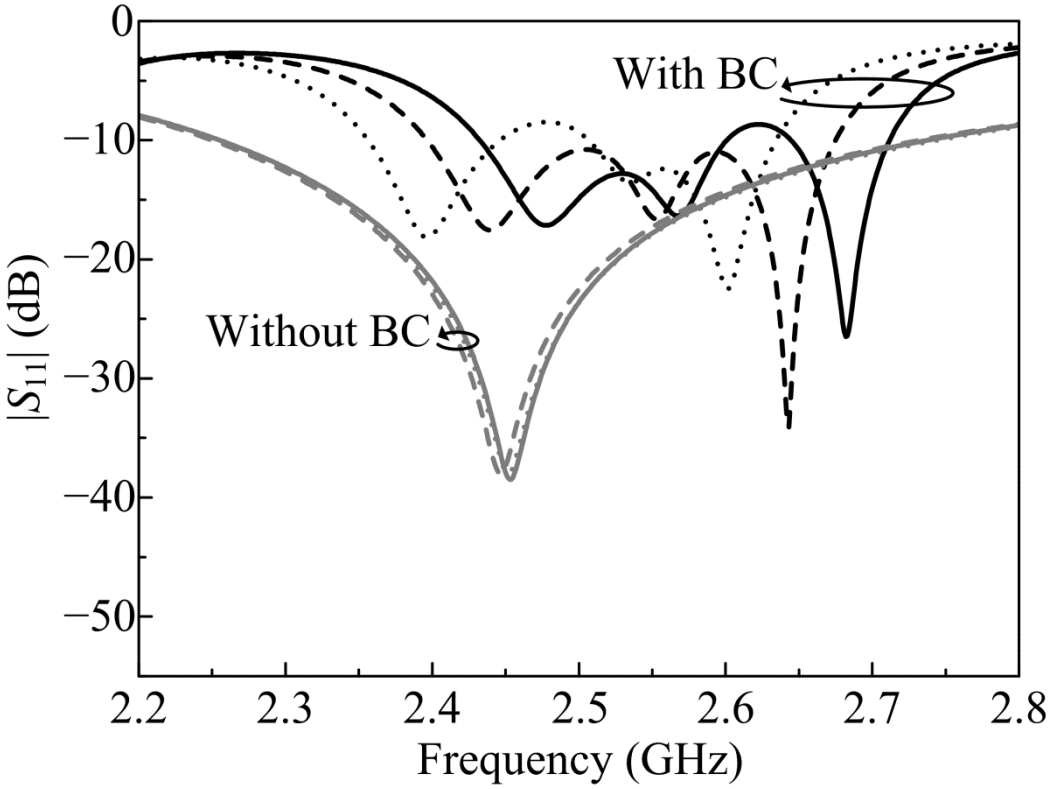

Fig. 2.15 Simulated input reflection coefficients with various L_1, L_2, and L_3. L_1:L_2:L_3 = 1:0.959:0.988. Black line: with BC. Gray line: without BC. Solid line: L_1 = 29 mm, L_2 = 27.82 mm, and L_3 = 28.65 mm. Dashed line: L_1 = 29.5 mm, L_2 = 28.3 mm, and L_3 = 29.15 mm. Dotted line: L_1 = 30 mm, L_2 = 28.78 mm, and L_3 = 29.64 mm.

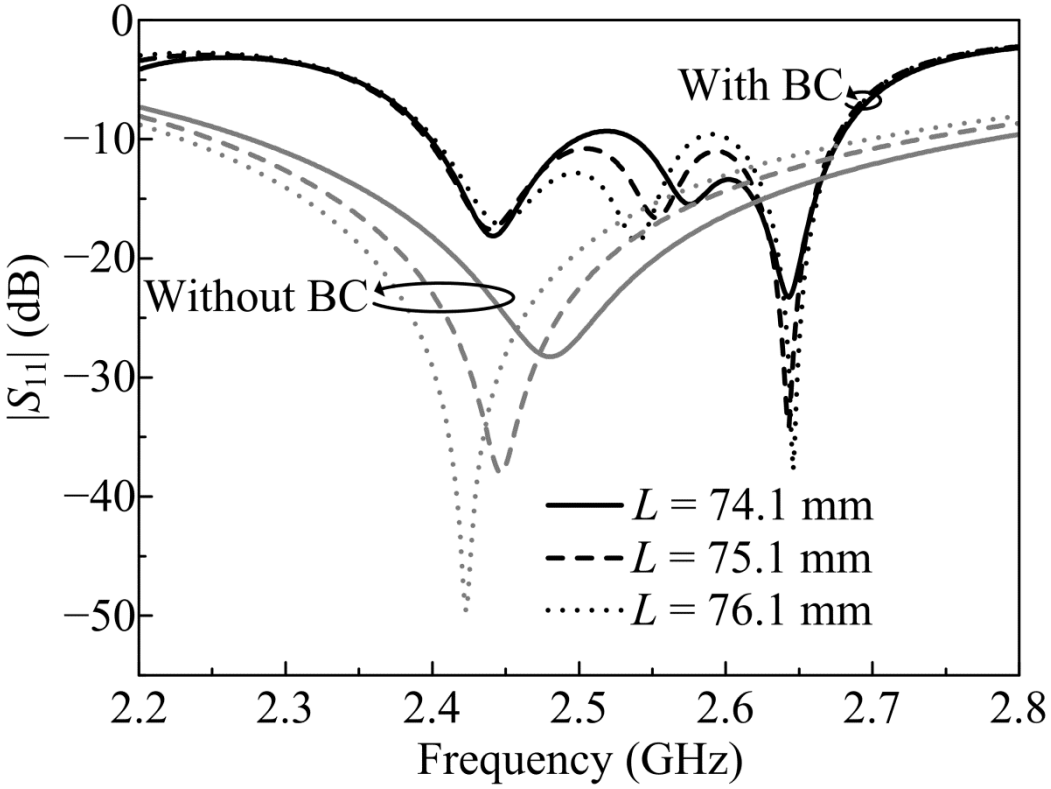

Fig. 2.16 Simulated input reflection coefficients with various *L*. Black line: with BC. Gray line: without BC.

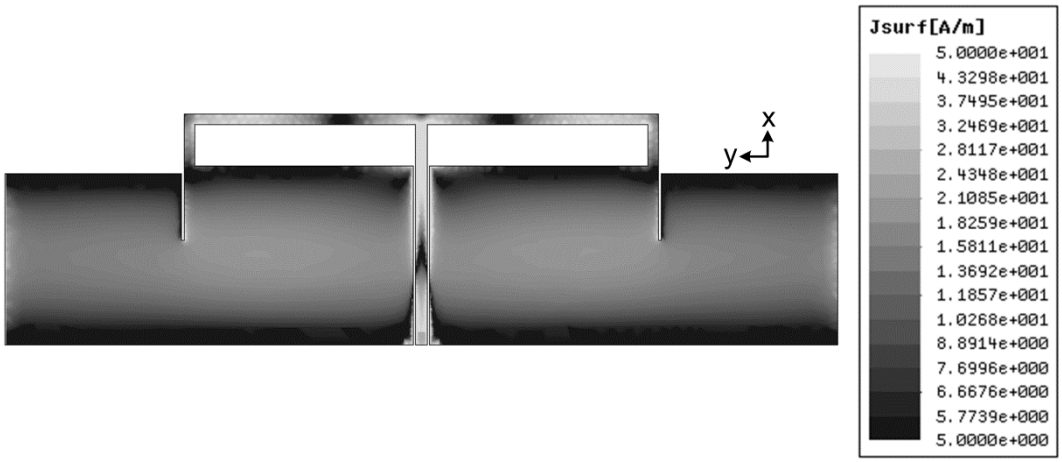

Fig. 2.17 Simulated surface electric current distribution for the antenna with BC at 2.45 GHz.

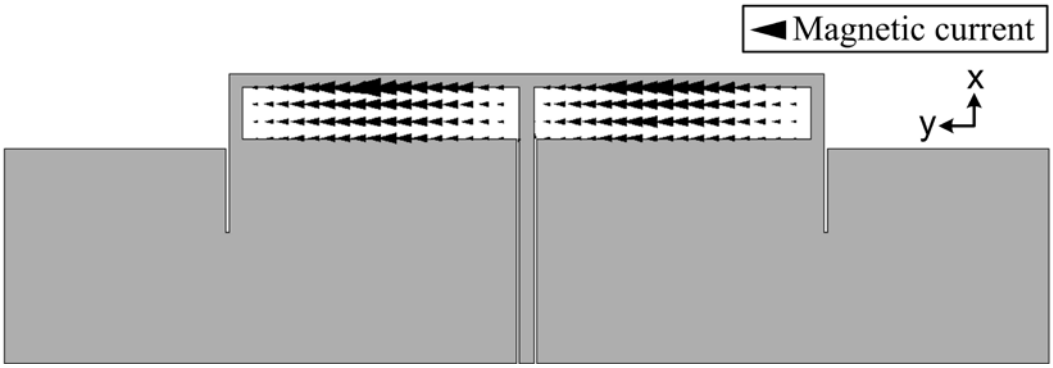

Fig. 2.18 Simulated equivalent magnetic current distribution in the slot dipole of the antenna without BC at 2.45 GHz.

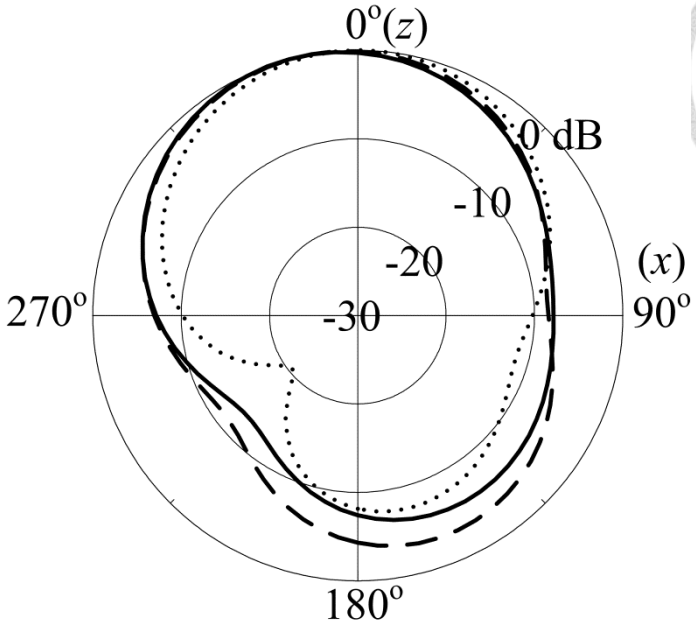

(a)

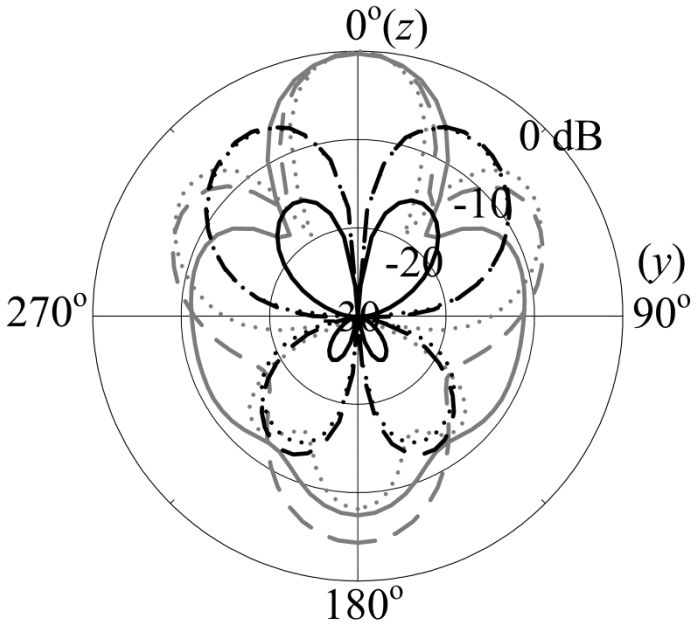

(b)

Fig. 2.19 Simulated radiation patterns of the antenna with BC. (a) E-plane (*x*-*z* plane) and (b) H-plane (*y*-*z* plane). Black line: E_θ. Gray line: E_ϕ. Solid line: 2.45 GHz. Dashed line: 2.55 GHz. Dotted line: 2.65 GHz.

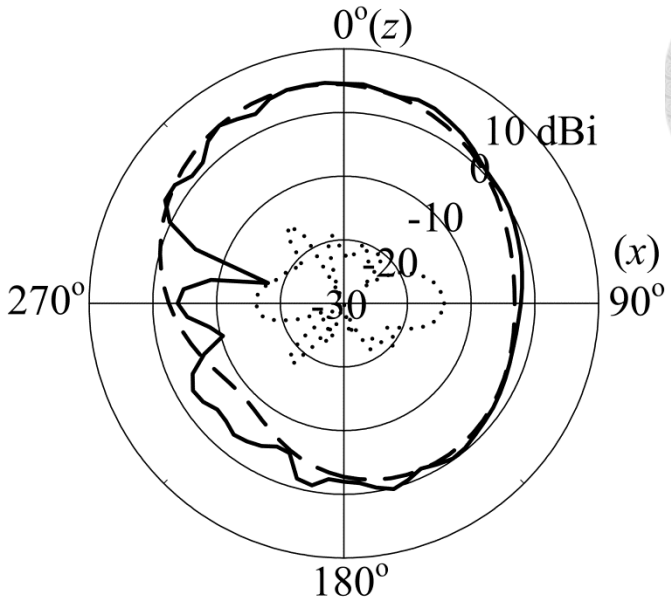

(a)

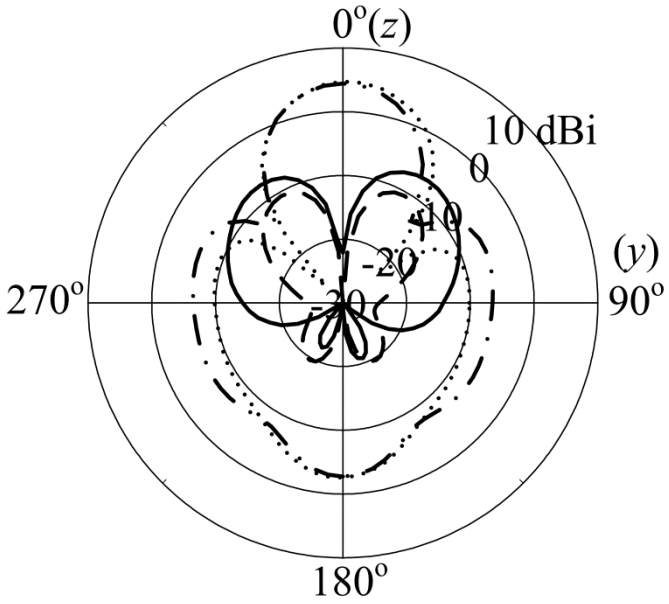

(b)

Fig. 2.20 Gain patterns of the antenna with BC at 2.45 GHz. (a) E-plane (*x*-*z* plane) and (b) H-plane (*y*-*z* plane). Solid line: measured E_θ. Dashed line: simulated E_θ. Dotted line: measured E_ϕ. Dash-dotted line: simulated E_ϕ.

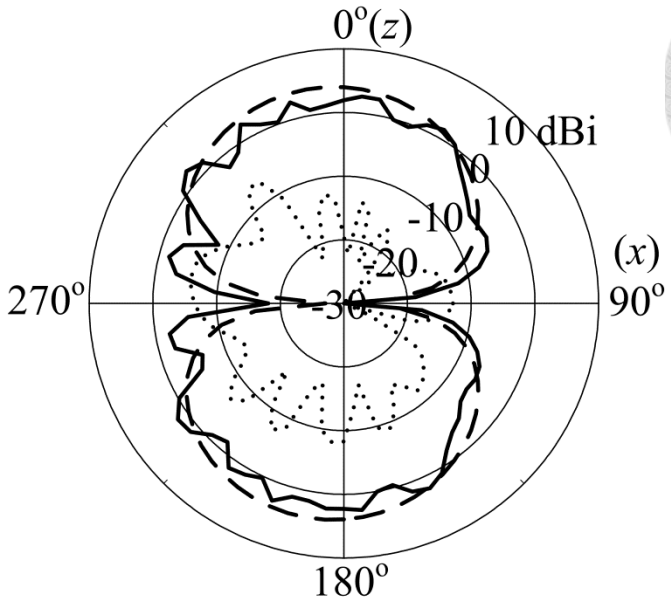

(a)

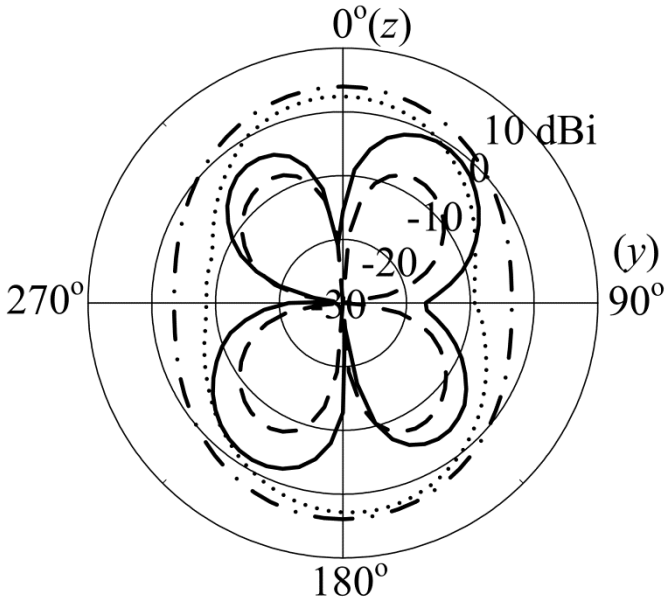

(b)

Fig. 2.21 Gain patterns of the antenna without BC at 2.45 GHz. (a) E-plane (*x*-*z* plane) and (b) H-plane (*y*-*z* plane). Solid line: measured E_θ. Dashed line: simulated E_θ. Dotted line: measured E_ϕ. Dash-dotted line: simulated E_ϕ.

TABLE II

SIMULATED AND MEASURED ANTENNA GAINS AND RADIATION EFFICIENCIES AT 2.45 GHZ

	Without BC		With BC	
	Sim.	Meas.	Sim.	Meas.
Antenna gain (dBi)	4.1	3.7	4.6	5.1
Radiation efficiency (%)	90.8	82.5	42.5	49.9

Chapter 3

Design of an EBG-Backed Coplanar Waveguide-Fed Slot Dipole Antenna

Design of an electromagnetic bandgap (EBG)-backed coplanar waveguide (CPW)-fed slot dipole antenna is presented. The antenna is formed by placing a CPW-fed slot dipole on the top of the EBG structure. It is found that the design considerations of the EBG-backed CPW-fed slot dipole are different from those of the conventional CPW-fed slot dipole. This is because the propagation characteristics of the EBG-backed slotline utilized in the EBG-backed design are quite different from those of the slotline for conventional design. By using the extracted propagation constant of the EBG-backed slotline, a detailed antenna design procedure is presented. The proposed antenna is designed, fabricated, and tested. Simulation and measurement results are presented and discussed.

3.1 INTRODUCTION

In microwave printed circuit applications, it is very tempting to introduce a back conductor, a conducting sheet, to the slotline or coplanar waveguide (CPW). The conductor-backed slotline (CBS) and conductor-backed CPW (CBCPW) have several

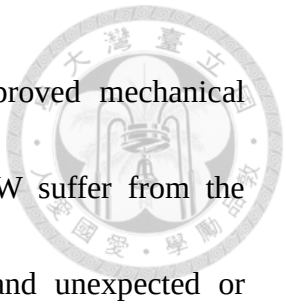

advantages such as help in grounding floating regions and improved mechanical strength and heat sink capability. However, the CBS and CBCPW suffer from the parallel-plate mode leakage problem, causing additional losses and unexpected or unwanted coupling to neighboring line in printed circuits [27]. The parallel-plate mode leakage problem also exists in a conductor-backed slot antenna design, when the back conductor is used to render the radiation of slot antenna from bi-directional to uni-directional [101], [103]. The unwanted parallel-plate mode would drastically degrade the antenna performance of the conductor-backed slot.

To solve the parallel-plate mode leakage problem, an electromagnetic bandgap (EBG) structure can be used to inhibit the propagation of parallel-plate mode within a limited frequency band, called bandgap or stopband [139], [140]. In [101] and [103], when compared with the conductor-backed slot antenna, the EBG-backed slot antenna design has shown improved antenna gain and efficiency. In addition, the EBG-backed two slot antennas have demonstrated improved isolation between the two slots and better diversity gain, compared with the conductor-backed two slot antennas. However, there were almost no discussions about the design procedure for the EBG-backed slot antenna and the relation between the EBG-backed slot antenna and an EBG-backed slotline, especially the characteristics of the EBG-backed slotline.

In the authors' preliminary work [141], the simulated and measured results of the

EBG-backed slot dipole antenna and slotline are presented. The propagation constant (β) of the EBG-backed slotline is extracted by using its one-period scattering parameters; however, the mutual coupling in the EBG-backed slotline is not taken into account. In this chapter, a further study of [141] is presented. First, the β of the EBG-backed slotline is simulated with considering the mutual coupling in the EBG-backed slotline. In addition, an equivalent circuit model of the EBG-backed slotline is presented and discussed. According to the extracted β, the detailed design procedure for the EBG-backed CPW-fed slot dipole antenna is proposed and the relation between the antenna and the EBG-backed slotline is clearly explained. Next, the input admittance and the current distribution of the antenna are simulated and discussed. Finally, the radiation characteristics of the antenna are compared with those of the CBCPW-fed slot dipole antenna and conventional CPW-fed slot dipole antenna.

3.2 ANTENNA STRUCTURE AND DESIGN

Fig. 3.1 shows the geometry of the EBG-backed CPW-fed slot dipole antenna. Three metal layers are plotted in Fig. 3.1(a)–(c), respectively, and two inter-layer substrates are indicated in the cross sectional view of the structure (Fig. 3.1(d)). The light and dark gray areas represent the substrate and metal parts, respectively, while the black areas, shown in Fig. 3.1(b)–(d), represent the blind cylindrical vias, connecting

the center and bottom metals.

Fig. 3.1(a) shows that a slot dipole of arm length L_S and width W_S inductively fed by a CPW of strip width S, gap width G, and length L_f. Fig. 3.1(b) shows an enlargement of a square mushroom-type EBG unit cell with unit-cell length P_{EBG}, square metal patch length W_{EBG}, and blind via diameter D in the center metal layer. Each blind via is placed symmetrically in the center of each square metal patch.

To design the EBG-backed CPW-fed slot dipole antenna of operating at the fundamental resonant frequency (f_0), the dimensions of the mushroom-type EBG structure should be determined first. The center frequency of the stopband of the mushroom-type EBG is chosen around f_0. Second, the arm length of slot dipole L_S equals to approximately a half λ_g, where λ_g is the guided-wavelength of the EBG-backed slotline at f_0. Within the stopband of the mushroom-type EBG structure, the EBG-backed slotline mode has a cutoff frequency (f_C), which will be shown in the next section. For frequency < f_C, the mode is nonpropagating, while for frequency > f_C, the mode propagates. Thus, the slot width W_S should be carefully chosen to achieve good input match and have f_0 above f_C.

3.3 SIMULATION AND MEASUREMENT RESULTS

In this chapter, full-wave simulations were carried out by using ANSYS HFSS ver. 13. The proposed antenna is designed on the FR-4 substrates with dielectric constant ε_r = 4.2, loss tangent tanδ = 0.02, and height h = 0.8 mm. f_0 is chosen at 5 GHz. By using the method described in [140], P_{EBG}, W_{EBG}, and D are determined to be 6.5, 6.2, and 0.6 mm, respectively. The stopband of the mushroom-type EBG structure designed ranges from 3.68 to 6.58 GHz, the center frequency of which is around f_0.

To effectively suppress the parallel-plate mode in the substrates, the EBG-backed slot dipole on the top metal layer are located in the middle of ten columns of mushroom-type EBG structure as shown in Fig. 3.1 so that the total width of the structure W is $10P_{EBG}$ (65 mm). A section of the EBG-backed slotline is cut from Fig. 3.1 and re-drawn in Fig. 3.2. The horizontal dotted lines in Fig. 3.2(a)–(c) mark a period of the EBG-backed slotline and its period length is the same as the mushroom-type EBG unit-cell length P_{EBG}. For one period of the EBG-backed slotline, it can be seen that the slotline etched on the top metal layer provides series inductance L_S and shunt capacitance C_S, while the loading effect of EBG structure on the slotline can be modeled as a shunt circuit, composed of C_{p1}, C_{p2}, and L_v. Thus, an equivalent circuit model of a

one-period EBG-backed slotline structure is derived and plotted in Fig. 3.3. By using the analysis procedure for infinite periodic structures described in [142, sec. 8.1], β of the equivalent circuit model can be derived as following:

$$\beta = \frac{1}{P_{EBG}} \cos^{-1}\left(1 + \frac{Z_1 + Z_2}{2Z_3}\right) \tag{3.1}$$

where

$$Z_1 = j\omega L_S = Z_2$$

$$Z_3 = \frac{1}{j\omega C_S + \dfrac{1}{\dfrac{1}{j\omega C_{p1}} + \dfrac{1}{j\omega C_{p2} + \dfrac{1}{j\omega L_v}}}}.$$

When β in (3.1) is equal to zero, f_C of the EBG-backed slotline mode can be given by

$$f_C = \frac{\omega_C}{2\pi} = \frac{1}{2\pi}\sqrt{\frac{C_{p1} + C_S}{L_v\left[C_{p1}C_{p2} + (C_{p1} + C_{p2})C_S\right]}}. \tag{3.2}$$

The EBG-backed slotline width W_S is chosen to be 0.3 mm. With consideration of the mutual coupling in the EBG-backed slotline, the modal analysis for the β of EBG-backed slotline mode is carried out by using HFSS and the associated simulation setup described in [143]. The β of equivalent circuit model shown in Fig. 3.3 is calculated by using (3.1), together with circuit values (L_S = 0.3 nH, C_S = 0.896 pF, C_{p1} = 1.78 pF, C_{p2} = 1.77 pF, and L_v = 0.47 nH). For comparison, the geometry of a conventional slotline is plotted in Fig. 3.4 and its β is evaluated by using closed-form

expressions in [144]. Fig. 3.5 shows β's of the slotlines with and without back EBG structure. It can be clearly seen that the β's of the EBGB slotline are quite different from that of the conventional slotline due to the back EBG structure. Compared with the conventional slotline, the EBG-backed slotline has higher dispersion because of the loading effect of EBG structure. The β's of the EBG-backed slotline extracted by using HFSS and derived from the equivalent circuit model are in good agreement. f_C of the EBG-backed slotline calculated via (3.2) is roughly 4.772 GHz. f_C is below f_0 (5 GHz), as desired. At f_0, the extracted β of the EBG-backed slotline is roughly 73.2 rad/m. The corresponding λ_g is about 85.8 mm. Because of the parasitic effects of short-ended terminals of the slot dipole, L_S is chosen to be 39 mm, which is approximately $0.45\lambda_g$, a little smaller than $0.5\lambda_g$ in this design. The S and G of the 50-Ω EBG-backed CPW are chosen to be 2 and 0.9 mm, respectively. The other geometric parameters used are: L_f = 32.35 mm and L = 91 mm.

The EBG-backed CPW-fed slot dipole antenna was simulated and fabricated by using the designed geometric parameters, which are summarized in Table III. Fig. 3.6 shows the measured and simulated input reflection coefficients of the proposed antenna. The measured and simulated f_0's are 4.93 and 5 GHz, respectively. The discrepancies between measured and simulated results may be due to the manufacturing tolerances. The measured and simulated impedance bandwidths ($|S_{11}| \leq -10$ dB) are 4% (4.83–5.03

GHz) and 3.8% (4.91–5.1 GHz), respectively.

By de-embedding the attached EBG-backed CPW, input admittance of the EBG-backed CPW-fed slot dipole antenna is simulated at the reference plane marked in Fig. 3.1(a). The frequency response of the input admittance is plotted in Fig. 3.7. The fundamental mode resonates at 5 GHz, as predicted, while the first higher-order mode resonates at 5.96 GHz, not roughly two times of the fundamental resonant frequency. This is because the EBG-backed slotline has higher dispersion. The input admittance of the fundamental resonant mode is close to 0.02 S (characteristic admittance of the transmission line G_0 = 1/50 S) and well-matched at 5 GHz, while the input admittance of the first higher order mode is too large to be matched at 5.96 GHz. The results are consistent with the simulated input reflection coefficient shown in Fig. 3.6.

Fig. 3.8 shows instantaneous electric current distributions simulated at 5 GHz. Each arm of the slot dipole has half-wavelength resonance, as predicted. In addition, it can be seen that the parallel-plate mode leakage problem is solved because most of the currents are concentrated around the CPW-fed slot dipole.

The measured and simulated E- and H-plane radiation patterns at 4.93 GHz are shown in Fig. 3.9(a) and (b), respectively. The E- and H-planes are *x*-*z* and *y*-*z* planes, respectively. The main beam of the antenna points in the broadside direction (+z or θ = 0° direction). The front-to-back ratio is roughly 13 dB. Thus, a satisfactorily

uni-directional radiation pattern is achieved. It can be observed that the smooth E-plane co-polarization pattern is obtained because of eliminating the parallel-plate mode propagation in the underlying geometry and the relevant radiation from the edges of the plates. The simulated cross-polarization components in both planes are invisible because they are lower than −29.4 dB, which is very close to the lower bound (−30 dB) of the radial axis. The measured cross-polarization levels are below −16 dB in all directions. The measured radiation patterns agree well with the simulated ones. The measured and simulated antenna gains are 7.8 and 6.1 dBi, respectively. The simulated radiation efficiency is 49.8% and it is a little low due to the lossy FR-4 substrate used. If the simulated loss tangent of FR-4 substrate is reduced from 0.02 to 0.002, the simulated radiation efficiency increases from 49.8% to 85.6%. Thus, radiation efficiency can be improved by using low-loss substrate. By using the method discussed in [145], the measured radiation efficiency is found to be 60.8%. By using the proposed design procedure, the EBG-backed CPW-fed slot dipole antenna can be designed to have good impedance matching, moderate antenna gain, and uni-directional radiation pattern without suffering parallel-plate mode leakage problem.

It is noted that the location of the slot dipole with respect to the EBG structure would alter the guided-wavelength of EBG-backed slotline, so that L_S and W_S for the optimized antenna design would be different. As long as the proposed design procedure

is used, the optimized designs for the EBG-backed slot dipole at different locations can be easily obtained.

For comparison, the optimum designs of CBCPW-fed slot dipole antenna (without EBG structure) and conventional CPW-fed slot dipole antenna (without EBG structure and back conductor) are also simulated at 5 GHz. The simulated slot lengths are 39 and 17.8 mm, respectively, the simulated impedance bandwidths are 6.4% and 18.8%, respectively, the simulated radiation efficiencies are 20.5% and 88.3%, respectively, and the simulated antenna gains are −0.5 and 6.2 dBi, respectively. For a bi-directionally radiated slot antenna, the conventional CPW-fed slot dipole is a good choice. For a uni-directionally radiated slot antenna, the simulated radiation efficiency and antenna gain of the EBG-backed CPW-fed slot dipole antenna are 49.9% and 6.3 dBi, which is larger than those of the CBCPW-fed slot antenna due to the suppression of the unwanted parallel-plate mode. Although the impedance bandwidth of the EBG-backed CPW-fed slot dipole antenna is a little smaller than that of the CBCPW-fed slot antenna, the back EBG structure is a good option to render the radiation of CPW-fed slot dipole antenna from bi-directional to uni-directional.

3.4 CONCLUSION

Design of an EBG-backed CPW-fed slot dipole antenna has been presented. A

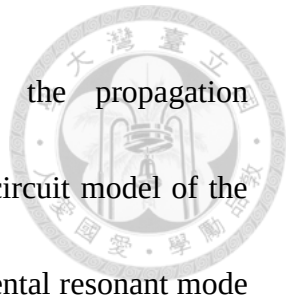

detailed antenna design procedure is constructed by using the propagation characteristics of the EBG-backed slotline. In addition, equivalent circuit model of the EBG-backed slotline has been proposed and discussed. The fundamental resonant mode of the antenna has been designed to operate at the desired frequency and it is verified by looking into the simulated input admittance and current distribution. Without suffering the parallel-plate mode leakage problem, the antenna has been shown to achieve good impedance matching and satisfactory antenna performance for uni-directional radiation.

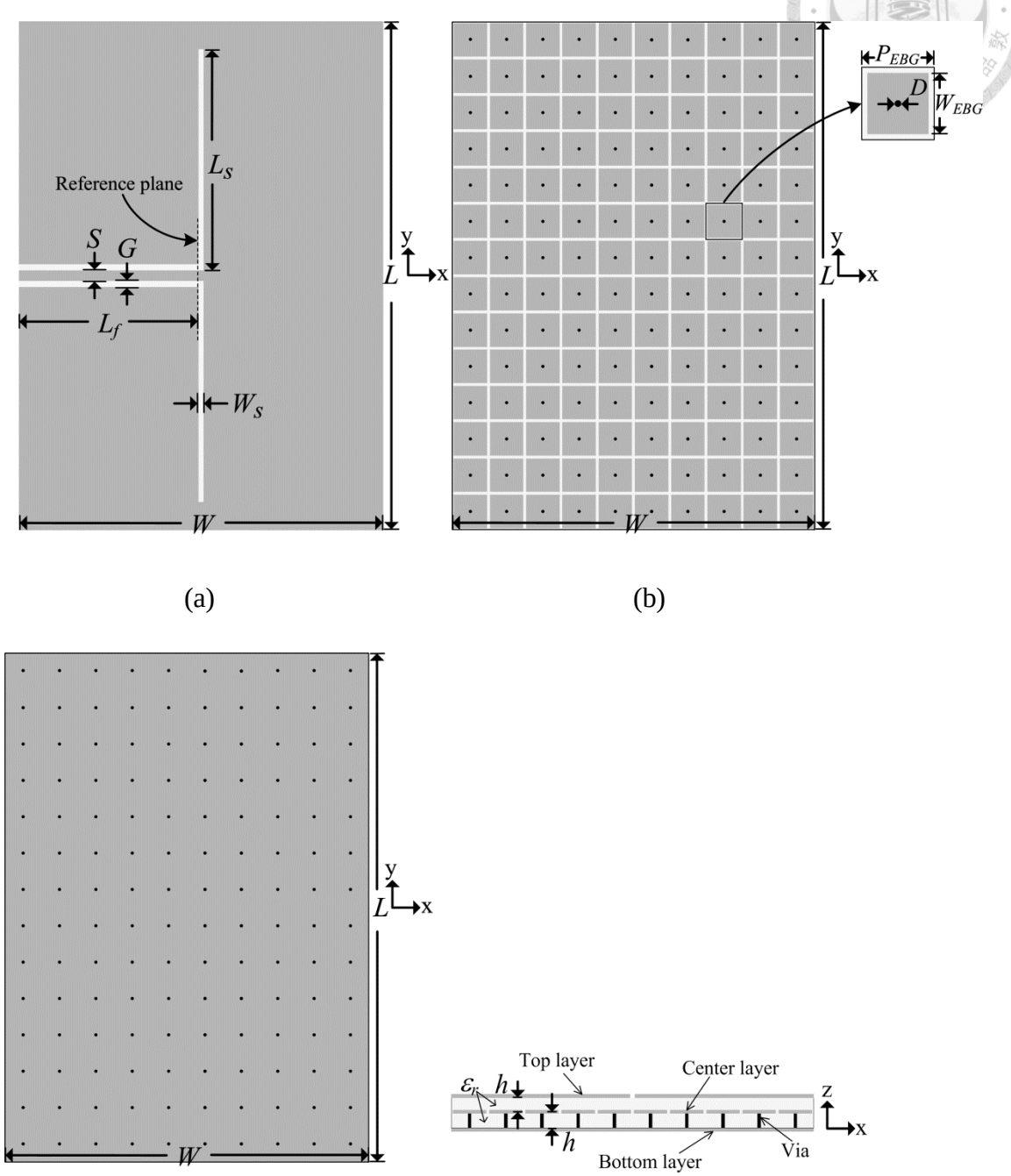

Fig. 3.1 Geometry of the EBG-backed CPW-fed slot dipole antenna. (a) Top, (b) center, and (c) bottom layers. (d) Cross-sectional view.

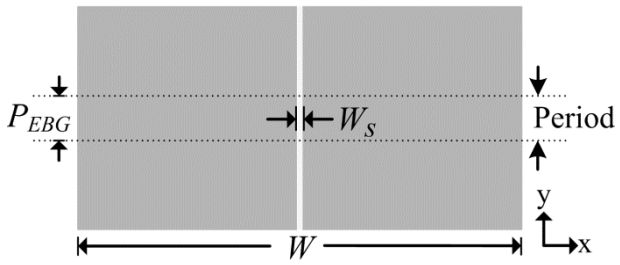

(a)

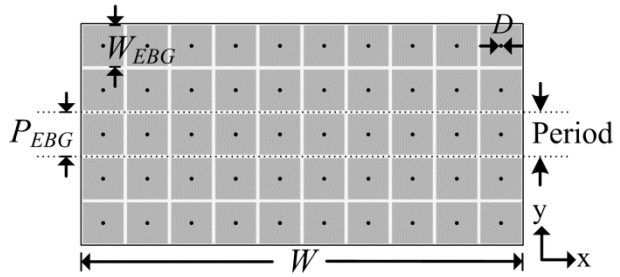

(b)

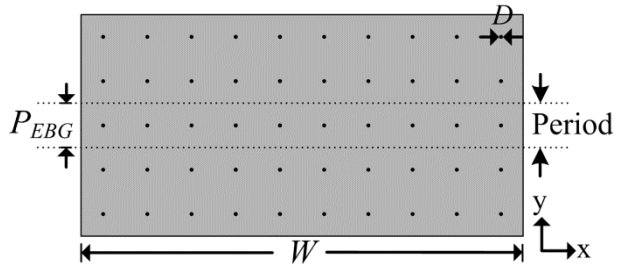

(c)

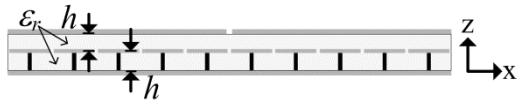

(d)

Fig. 3.2 Geometry of a five-period EBG-backed slotline. (a) Top, (b) center, and (c) bottom layers. (d) Cross-sectional view.

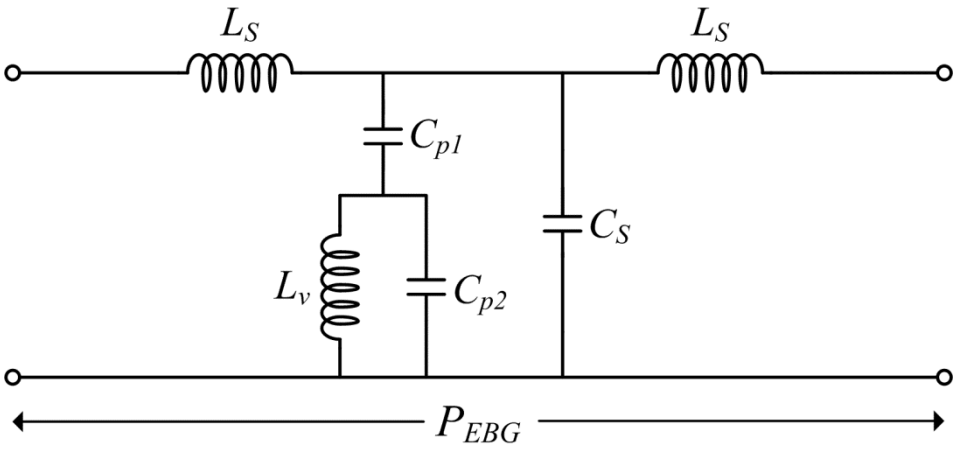

Fig. 3.3 Equivalent circuit model of the one-period EBG-backed slotline.

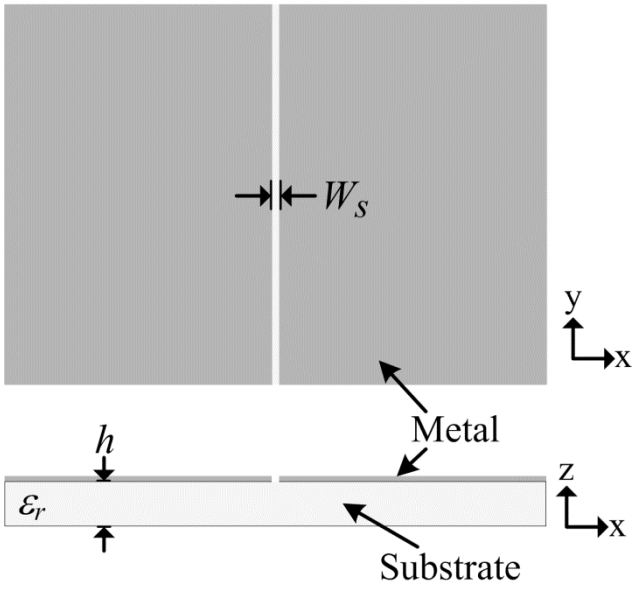

Fig. 3.4 Geometry of the conventional slotline. W_S = 0.3 mm, h = 1.6 mm, and ε_r = 4.2.

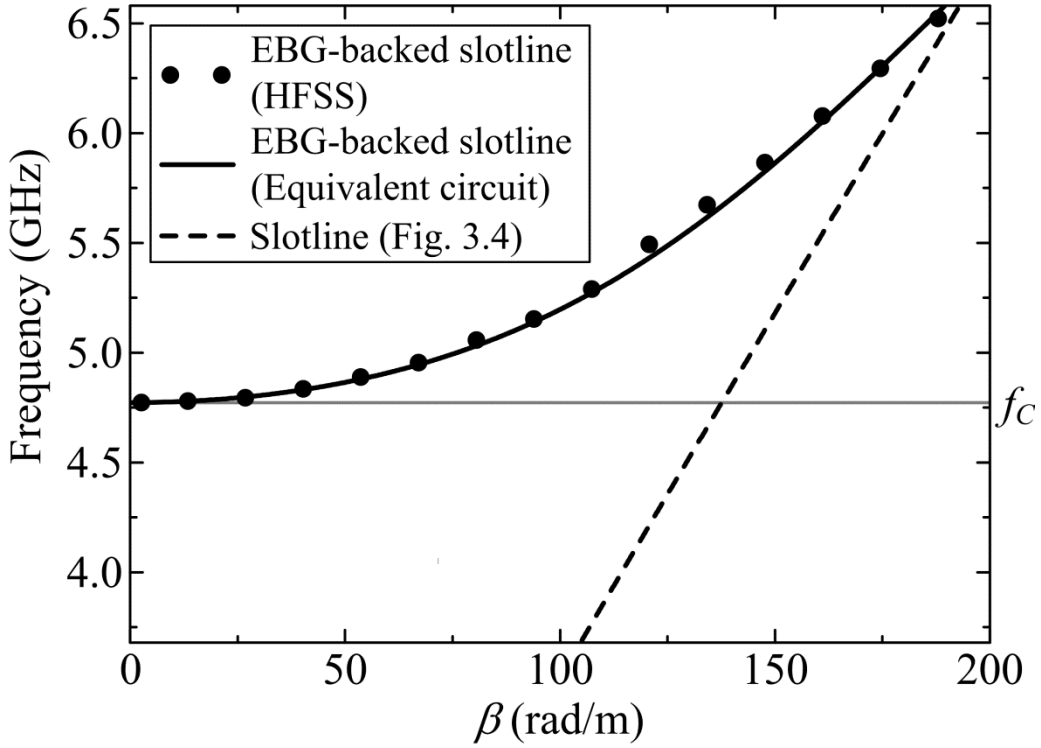

Fig. 3.5 β's of slotlines with and without back EBG structure.

TABLE III

GEOMETRIC PARAMETERS OF THE EBG-BACKED CPW-FED SLOT DIPOLE ANTENNA

P_{EBG}	W_{EBG}	D	W	W_S	L_S
6.5	6.2	0.6	65	0.3	39
L	S	G	L_f	h	Unit
91	2	0.9	32.35	0.8	mm

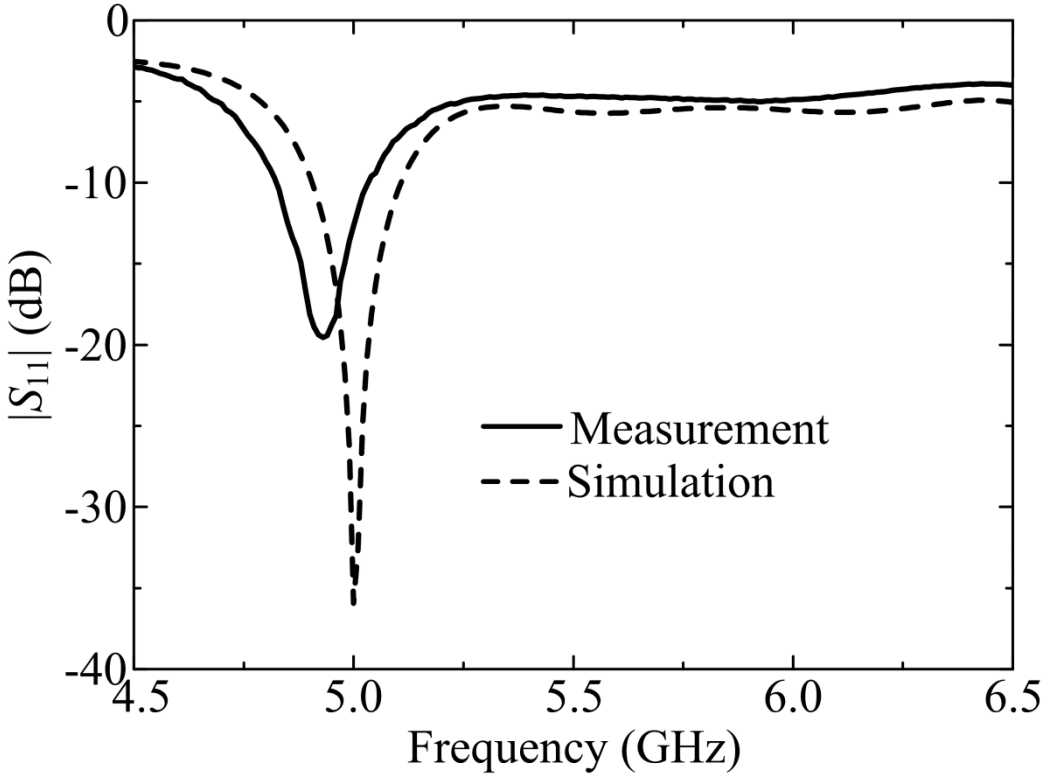

Fig. 3.6 Measured and simulated input reflection coefficients of the proposed antenna.

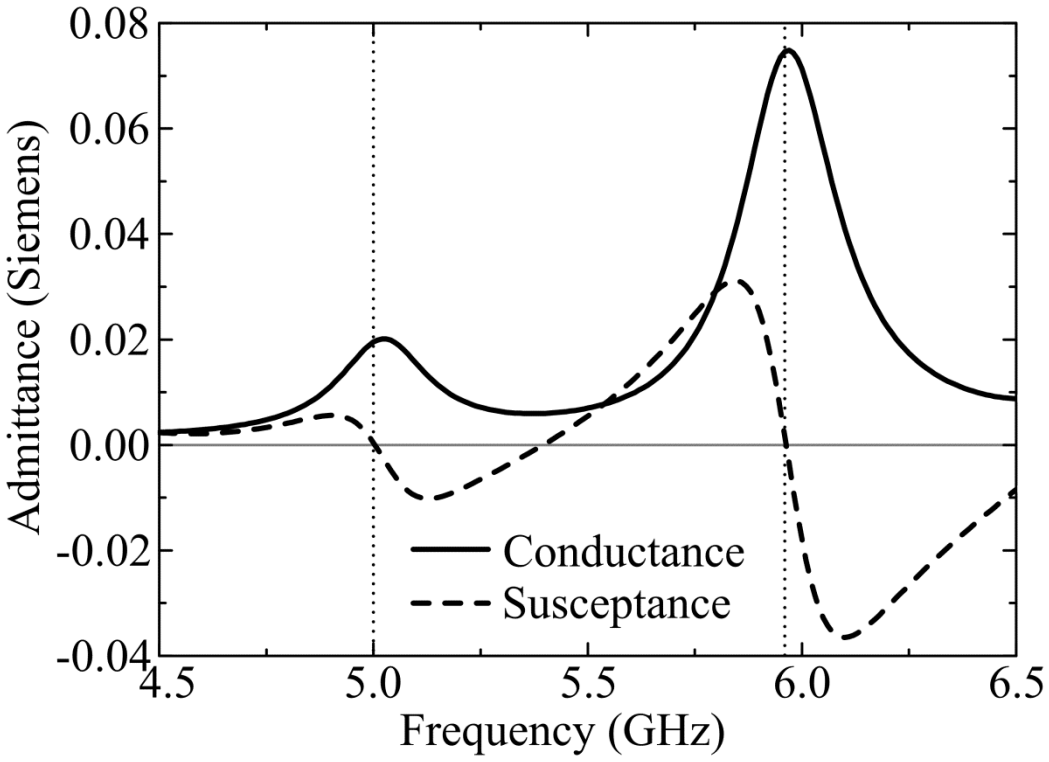

Fig. 3.7 Input admittance of the proposed antenna simulated at the reference plane marked in Fig. 3.1(a).

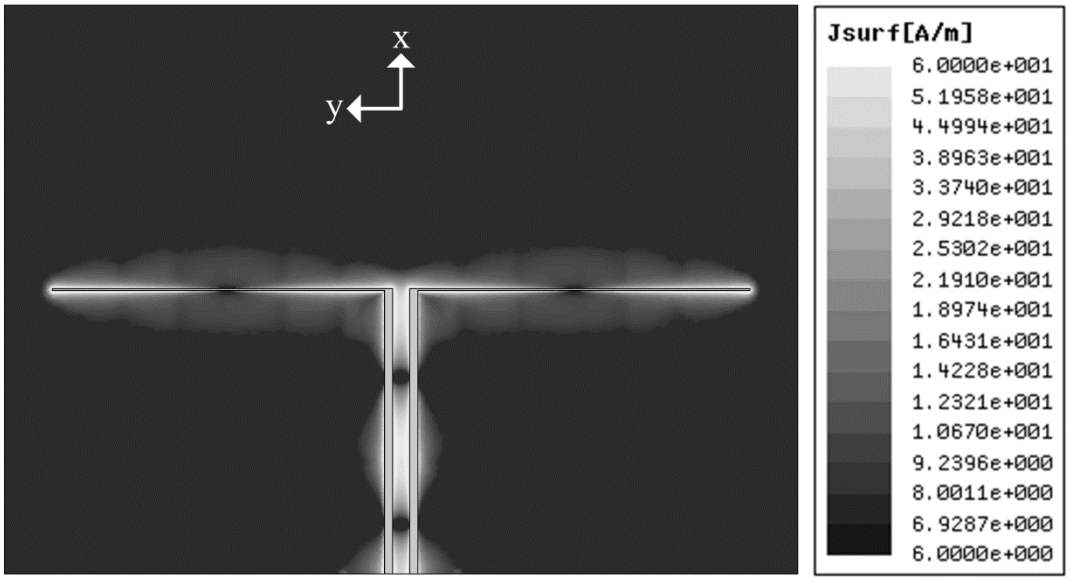

Fig. 3.8 Simulated electric current distribution on the top metal layer at 5 GHz.

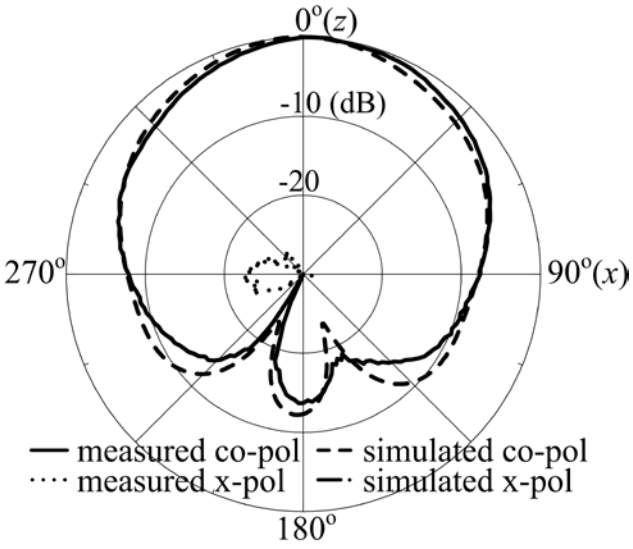

(a)

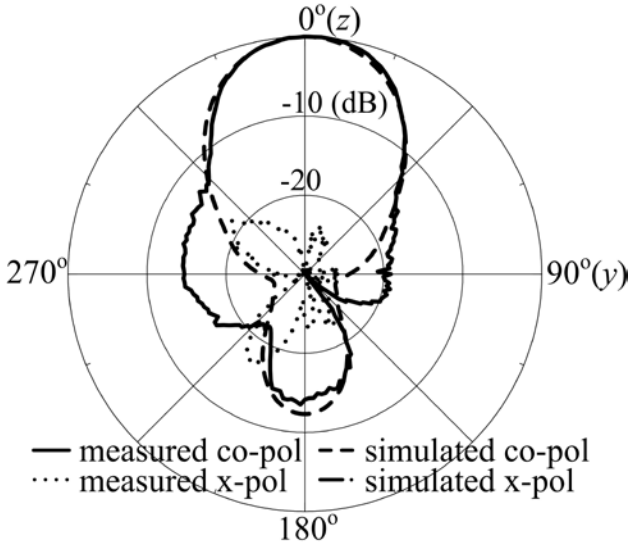

(b)

Fig. 3.9 Measured and simulated radiation patterns at 4.93 GHz. (a) E-plane (*x*-*z* plane). (b) H-plane (*y*-*z* plane). Co-pol: co-polarization. X-pol: cross-polarization.

Chapter 4

Conclusion

Designs of printed antenna fed by CPW with different backing materials have been presented in this dissertation. The first part of this dissertation includes three hybrid designs of printed antenna fed by CPW with and with BC. Each of them uses only one dielectric layer and is etched on one metal plate. In practical applications, when an antenna is integrated with a transceiver circuitry on the same printed circuit board, whether or not the system ground plane can be extended to the region under the antenna depends on the antenna having a backplane or not. If the integrating antenna is a hybrid one, as the one we have proposed, then the answer to the above question no longer depends on the antenna design, instead it depends now on the system requirements, such as the reduction of human body effect, improvement of heat sink capability and/or mechanical strength, having more available space for placing components/devices under the antenna, and etc. In the second part, design of an EBG-backed CPW-fed slot dipole antenna has been presented and analyzed. Detailed analysis and design have also been presented.

In Chapter 2, first, an original hybrid design of CPW-fed printed antenna with and without BC has been presented. An E-shaped strip protruded from the signal strip of the

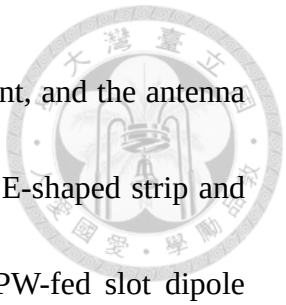

feed line is used to feed the side plane conductors when BC is present, and the antenna is a CBCPW-fed side plane patch antenna. When BC is absent, the E-shaped strip and the side planes form a slot dipole, and the antenna becomes a CPW-fed slot dipole antenna. Both the patch antenna with BC and the slot dipole antenna without BC are designed to operate at the same frequency with the same geometric parameters. The measured overlapping impedance bandwidth between the two antennas is 3.2%. Resonant behaviors and radiation characteristics of the hybrid antenna with and without BC have been shown to have satisfactory results and, indeed, it can adapt itself to the presence or absence of BC with good antenna performance.

In the second section of Chapter 2, a compact hybrid design of CPW-fed printed antenna with and without BC has been presented. A Γ-shaped strip protruded from the signal strip of the feed line is used to feed the right hand side of the plane conductor when BC is present, and the antenna is a CBCPW-fed side plane patch antenna. When BC is absent, the Γ-shaped strip and the right hand side plane form a half-wavelength slot, and the antenna becomes a CPW-fed half-wavelength slot antenna. Both the patch antenna with BC and the half-wavelength slot antenna without BC are designed to operate at the same frequency with the same geometric parameters. The measured overlapping impedance bandwidth between the two antennas is 2.5%. Compared with the original design, the compact design can achieve a 42% reduction in size.

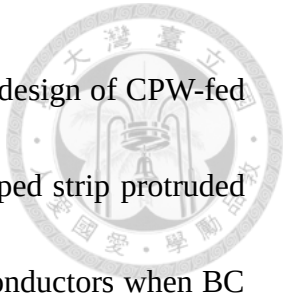

In the third section of Chapter 2, a bandwidth-enhanced hybrid design of CPW-fed printed antenna with and without BC has been presented. An E-shaped strip protruded from the signal strip of the feed line is used to feed the side plane conductors when BC is present, and the antenna is a bandwidth-enhanced CBCPW-fed side plane patch antenna. When BC is absent, the E-shaped strip and the side planes form a slot dipole, and the antenna becomes a CPW-fed slot dipole antenna. Both the bandwidth-enhanced patch antenna with BC and the slot dipole antenna without BC are designed to operate at the same frequency with the same geometric parameters. The measured overlapping impedance bandwidth between the two antennas is 9.9%, which is wide enough for most of the wireless communications. Also, the overlapping is roughly three times wider than the ones of the original and compact designs.

In Chapter 3, design of an EBG-backed CPW-fed slot dipole antenna has been presented. A detailed antenna design procedure is constructed by using the propagation characteristics of the EBG-backed slotline. In addition, an equivalent circuit model of the EBG-backed slotline has been proposed and discussed. The fundamental resonant mode of the antenna has been designed to operate at the desired frequency and it is verified by looking into the simulated input admittance and current distribution. Without suffering the parallel-plate mode leakage problem, the antenna has been shown to achieve good impedance matching and satisfactory antenna performance for

uni-directional radiation.

Reference

[1] C. P. Wen, “Coplanar waveguide: a surface strip transmission line suitable for nonreciprocal gyromagnetic device applications,” *IEEE Trans. Microw. Theory Tech.*, vol. MTT-17, no. 12, pp. 1087–1090, Dec. 1969.

[2] R. N. Simons, Coplanar Waveguide Circuits, Components, and Systems. New York: John Wiley & Sons, 2001.

[3] W. R. Deal, R. Tsai, M. D. Lange, J. B. Boos, B. R. Bennett, and A. Gutierrez, “A W-band InAs/AlSb low-noise/low-power amplifier,” *IEEE Microw. Wireless Compon. Lett.*, vol. 15, no. 4, pp. 208–210, Apr. 2005.

[4] A. Tessmann, I. Kallfass, A. Leuther, H. Massler, M. Kuri, M. Riessle, M. Zink, R. Sommer, A. Wahlen, H. Essen, V. Hum, M. Schlechtweg, and O. Ambacher, “Metamorphic HEMT MMICs and modules for use in a high-bandwidth 210 GHz radar,” *IEEE J. Solid-State Circuits*, vol. 43, no. 10, pp. 2194–2205, Oct. 2008.

[5] R. N. Simons and S. R. Taub, “Coplanar waveguide radial line double stub and application to filter circuits,” *Electron. Lett.*, vol. 29, no. 17, pp. 1584–1586, Aug. 1993.

[6] S.-N. Lee, J.-I. Lee, Y.-J. Kim, and J.-G. Yook, “Miniaturized CBCPW bandpass filter based on thin film polyimide on lossy silicon,” *IEEE Microw. Wireless Compon. Lett.*, vol. 16, no. 10, pp. 546–548, Oct. 2006.

[7] M. Nedil, A. Djaiz, and T.A. Denidni, “Ultra-wideband bandpass filter using back-to-back CBCPW-to-CBCPW transition,” *Electron. Lett.*, vol. 44, no. 5, pp. 362–363, Feb. 2008.

[8] Z. Yin and Z. Shao, “Design of a novel CBCPW-bandpass filter by using U-slot DGSs,” in *Proc. Int. Conf. Computational Problem-Solving*, Lijiang, China, Dec. 2010, pp. 293–295.

[9] J.-P. Raskin, G. Gauthier, L. P. Katehi, and G. M. Rebeiz, “Mode conversion at GCPW-to-microstrip-line transitions,” *IEEE Trans. Microw. Theory Tech.*, vol. 48, no. 1, pp. 158–161, Jan. 2000.

[10] R. Phltorak and M. Kitlinski, “Some remarks on the design of microstrip to coplanar line transformer,” in *Proc. Int. Conf. Microw., Radar and Wireless Comm.*, Warsaw, Poland, May 2004, pp. 836–839..

[11] Y. C. Lee and C. S. Park, “A compact and low-radiation CPW probe pad using CBCPW-to-microstrip transitions for V-band LTCC applications,” *IEEE Trans. Adv. Packag.*, vol. 30, no. 3, pp. 566–569, Aug. 2007.

[12] H.-H. Lee and J.-Y. Park, “Characterization of fully embedded RF inductors in organic SOP technology,” *IEEE Trans. Adv. Packag.*, vol. 32, no. 2, pp. 491–496, May. 2009.

[13] D.-H. Kwon, “A wideband balun and vertical transition between conductor-backed CPW and parallel-strip transmission line,” *IEEE Microw. Wireless Compon. Lett.*, vol. 16, no. 4, pp. 152–154, Apr. 2006.

[14] C.-F. Hung, A.-S. Liu, C.-H. Chien, C.-L. Wang, and R.-B. Wu “Bandwidth enhancement on waveguide transition to conductor backed CPW with high dielectric constant substrate,” *IEEE Microw. Wireless Compon. Lett.*, vol. 15, no. 2, pp. 128–130, Feb. 2005.

[15] W.-J. Lu, Y.-M. Bo, and H.-B. Zhu, “A broadband transition design for a conductor-backed coplanar waveguide and a broadside coupled stripline,” *IEEE Microw. Wireless Compon. Lett.*, vol. 22, no. 1, pp. 10–12, Jan. 2012.

[16] J. J. Lee, K. C. Eun, D. Y. Jung, and C. S. Park, “A novel GCPW to rectangular waveguide transition for 60 GHz applications,” *IEEE Microw. Wireless Compon. Lett.*, vol. 19, no. 2, pp. 80–82, Feb. 2009.

[17] H. Aliakbarian, S. Radiom, V. Tavakol, P. Reynaert, B. Nauwelaers, G.A.E. Vandenbosch, and G. Gielen, “Fully micromachined W-band rectangular

waveguide to grounded coplanar waveguide transition," *IET Microw. Antennas Propag.* , vol. 6, no. 3, pp. 533–540, Apr. 2012.

[18] I. Flammia, A. Stohr, C.C. Lenonhardt, J. Honecker, and A.G. Steffan, "71–76 GHz grounded CPW to WR-12 transition for quasi-hermetic RoF wireless transmitter," *Electron. Lett.*, vol. 48, no. 9, pp. 506–508, Apr. 2012.

[19] X.-P. Chen and K. Wu, "Low-loss ultra-wideband transition between conductor-backed coplanar waveguide and substrate integrated waveguide," in *IEEE MTT-S Int. Microw. Symp. Dig.*, Boston, USA, Jun. 2009, pp. 349–352.

[20] R.-Y. Fang, C.-F. Liu, and C.-L. Wang, "Compact and broadband CB-CPW-to-SIW transition using stepped-impedance resonator with 90°-bent slot," *IEEE Trans. Compon., Packag., Manuf. Technol.*, vol. 3, no. 2, pp. 247–252, Feb. 2013.

[21] Y. J. Cheng, X. Y. Bao, Y. X. Guo, "LTCC-based substrate integrated image guide and its transition to conductor-backed coplanar waveguide," *IEEE Microw. Wireless Compon. Lett.*, vol. 23, no. 9, pp. 450–452, Sep. 2013.

[22] I. Flammia, B. Khani, S. Arafat, and A. Stohr, "60 GHz grounded-coplanar-waveguide-to-substrate-integrated-waveguide transition for RoF transmitters," *Electron. Lett.*, vol. 50, no. 1, pp. 34–35, Jan. 2014.

[23] C. E. Bassey and G. R. Simpson, “A comparison of the coplanar waveguide (CPW) and conductor-backed coplanar waveguide (CBCPW) for use as aircraft ice sensors,” in *Proc. IEEE AP-S Int. Symp.*, Albuquerque, USA, Jul. 2006, pp. 821–824.

[24] C. Veyres and V. F. Hanna, “Extension of the application of conformal mapping techniques to coplanar lines with finite dimensions,” *Int. J. Electron.*, vol. 48, no. 1, pp. 47–56, Jan. 1980.

[25] Y. C. Shih and T. Itoh, “Analysis of conductor-backed coplanar waveguide,” *Electron. Lett.*, vol. 18, no. 12, pp. 538–540, Jun. 1982.

[26] R. W. Jackson, “Considerations in the use of coplanar waveguide for millimeter-wave integrated circuits,” *IEEE Trans. Microw. Theory Tech.*, vol. MTT-34, no. 12, pp. 1450–1456, Dec. 1986.

[27] H. Shigesawa, M. Tsuji, and A. A. Oliner, “Conductor-backed slot line and coplanar waveguide: dangers and full-wave analysis,” in *IEEE MTT-S Int. Microw. Symp. Dig.*, New York, USA, May 1988, pp. 199–202.

[28] L.-M. Chou, R. G. Rojas, and P. H. Pathak, “A WH/GSMT based full-wave analysis of the power leakage from conductor-backed coplanar waveguides,” in *IEEE MTT-S Int. Microw. Symp. Dig.*, Albuquerque, USA, Jun. 1992, pp. 219–222.

[29] W. E. McKinzie and N. G. Alexopoulos, “Leakage losses for the dominant mode of conductor-backed coplanar waveguide,” *IEEE Microw. Guided Wave Lett.*, vol. 2, no. 2, pp. 65–66, Feb. 1992.

[30] K. Beilenhoff and W. Heinrich, “Excitation of the parasitic parallel-plate line mode at coplanar discontinuities,” in *IEEE MTT-S Int. Microw. Symp. Dig.*, Denver, USA, Jun. 1997, pp. 1789–1792.

[31] M. Riaziat, I. J. Feng, R. Majidi-Ahy, and B. A. Auld, “Single-mode operation of coplanar waveguides,” *Electron. Lett.*, vol. 23, no. 24, pp. 1281–1283, Nov. 1987.

[32] R. W. Jackson, “Mode conversion at discontinuities in finite-width conductor-backed coplanar waveguide,” *IEEE Trans. Microw. Theory Tech.*, vol. 37, no. 10, pp. 1582–1589, Oct. 1989.

[33] C.-C. Tien, C.-K. C. Tzuang, S. T. Peng, and C.-C. Chang, “Transmission characteristics of finite-width conductor-backed coplanar waveguide,” *IEEE Trans. Microw. Theory Tech.*, vol. 41, no. 9, pp. 1616–1624, Sep. 1993.

[34] C.-C. Tien, C.-K. C. Tzuang, and S. T. Peng, “Effect of finite-width backside plane on overmoded conductor-backed coplanar waveguide,” *IEEE Microw. Guided Wave Lett.*, vol. 3, no. 8, pp. 259–261, Aug. 1993.

[35] W.-T. Lo, and C.-K. C. Tzuang, S.-T. Peng, C.-C. Tien, C.-C. Chang, and J.-W. Huang, “Resonant phenomena in conductor-backed coplanar waveguides (CBCPW’s),” *IEEE Trans. Microw. Theory Tech.*, vol. 41, no. 12, pp. 2099–2108, Dec. 1993.

[36] W. H. Haydl, “Resonance phenomena and power loss in conductor-backed coplanar structures,” *IEEE Microw. Guided Wave Lett.*, vol. 20, no. 12, pp. 514–516, Dec. 2000.

[37] R. N. Simons, G. E. Ponchak, K. S. Martzaklis, and R. R. Romanofsky, “Channelized coplanar waveguide: discontinuities, junctions, and propagation characteristics,” in *IEEE MTT-S Int. Microw. Symp. Dig.*, Long Beach, USA, Jun. 1989, pp. 915–918.

[38] R. N. Simons and G. E. Ponchak, “Coax-to-channelised coplanar waveguide in-phase n-way, radial power divider,” *Electron. Lett.*, vol. 26, no. 11, pp. 754–756, May 1990.

[39] R. N. Simons, “New channelised coplanar waveguide to rectangular waveguide post and slot couplers,” *Electron. Lett.*, vol. 27, no. 10, pp. 856–858, May. 1991.

[40] C.-C. Tien, C.-K. C. Tzuang, and J. Monroe, “Effect of lateral walls on the propagation characteristics of finite-width conductor-backed coplanar waveguides,” *Electron. Lett.*, vol. 29, no. 15, pp. 1357–1358, Jul. 1993.

[41] J.-G. Yook, N. I. Dib, and L. P. B. Katehi, “Characterization of high frequency interconnects using finite difference time domain and finite element methods,” *IEEE Trans. Microw. Theory Tech.*, vol. 42, no. 9, pp. 1727–1736, Sep. 1994.

[42] N. K. Das, “Two conductor-backed configurations of slotline or coplanar waveguide for elimination or suppression of the power-leakage problem,” in *IEEE MTT-S Int. Microw. Symp. Dig.*, San Diego, USA, May. 1994, pp. 153–156.

[43] N. K. Das, “Methods of suppression or avoidance of parallel-plate power leakage from conductor-backed transmission line,” *IEEE Trans. Microw. Theory Tech.*, vol. 44, no. 2, pp. 169–181, Feb. 1996.

[44] J. M. Johnson and Y. Rahmat-Samii, “The tab monopole,” *IEEE Trans. Antennas Propag.*, vol. 45, no. 1, pp. 187–188, Jan. 1997.

[45] G. E. Ponchak, D. Chun, J.-G. Yook, and L. P. B. Katehi, “The use of metal filled via holes for improving isolation in LTCC RF and wireless multichip packages,” *IEEE Trans. Adv. Packag.*, vol. 23, no. 1, pp. 88–99, Feb. 2000.

[46] W. H. Haydl, “On the use of vias in conductor-backed coplanar circuits,” *IEEE Trans. Microw. Theory Tech.*, vol. 50, no. 6, pp. 1571–1577, Jun. 2002.

[47] D. Deslandes and Ke Wu, “Analysis and design of current probe transition from grounded coplanar to substrate integrated rectangular waveguides,” *IEEE Trans. Microw. Theory Tech.*, vol. 53, no. 8, pp. 2487–2494, Aug. 2005.

[48] C. T.H. Lim, A. Ali, and J. S. Fu, “A broadband printed triangular monopole,” in *Proc*. *Asia-Pacific Microw. Conf.*, Suzhou, China, Dec. 2005.

[49] K. Ma, J. Ma, M. A. Do, and K. S. Yeo, “Experimentally investigating slow-wave transmission lines and filters based on conductor-backed CPW periodic cells,” in *IEEE MTT-S Int. Microw. Symp. Dig.*, Long Beach, USA, Jun. 2005, pp. 1653–1656.

[50] J. H. Choi and P. Russer, “The picosecond pulse transmission on the conductor-backed coplanar waveguide with via holes,” *IEEE Microw. Wireless Compon. Lett.*, vol. 16, no. 7, pp. 419–421, Jul. 2006.

[51] M. A. Habib, M. Nedil, and T. A. Denidni, “Radiation efficiency enhancement of slot antenna using EBG-pin inclusion,” in *Proc*. *IEEE AP-S Int. Symp.*, Albuquerque, USA, Jul. 2006, pp. 2295–2298.

[52] A. Patrovsky, M. Daigle, and K. Wu, “Coupling mechanism in hybrid SIW-CPW forward couplers for millimeter-wave substrate integrated circuits,” *IEEE Trans. Microw. Theory Tech.*, vol. 56, no. 11, pp. 2594–2601, Nov. 2008.

[53] G. D. Angelis, A. Lucibello, E. Proietti, R. Marcelli, and G. Bartolucci, “Design and technology of micro-machined coplanar grounded wave-guides,” *IET Microw. Antennas Propag.* , vol. 6, no. 5, pp. 497–504, Apr. 2012.

[54] K. Ma, K. S. Yeo, J.-G. Ma, “Phase compensation of cascaded conductor-backed CPW periodic cells,” *IEEE Trans. Compon., Packag., Manuf. Technol.*, vol. 2, no. 9, pp. 1455–1464, Sep. 2012.

[55] M. A. Magerko, L. Fan, and K. Chang, “Multiple dielectric structures to eliminate moding problems in conductor-backed coplanar waveguide MIC’s,” *IEEE Microw. Guided Wave Lett.*, vol. 2, no. 6, pp. 257–259, Jun. 1992.

[56] Y. Liu, K. Cha, and T. Itoh, “Elimination of resonance in finite-width conductor-backed coplanar waveguides,” in *Proc. 24th European Microw. Conf.*, Cannes, France, Sep. 1994, pp. 1222–1226.

[57] M. A. Magerko, L. Fan, and K. Chang, “Configuration considerations for multi-layered packaged conductor-backed coplanar waveguide MIC’s,” in *IEEE MTT-S Int. Microw. Symp. Dig.*, San Diego, USA, May. 1994, pp. 1697–1700.

[58] Y. Liu, K. Cha, and T. Itoh, “Non-leaky coplanar (NLC) waveguides with conductor backing,” *IEEE Trans. Microw. Theory Tech.*, vol. 43, no. 5, pp. 1067–1072, May 1995.

[59] C.-Y. Lee, Y. Liu, and T. Itoh, “The effects of the coupled slotline mode and air-bridges on CPW and NLC waveguide discontinuities,” *IEEE Trans. Microw. Theory Tech.*, vol. 43, no. 12, pp. 2759–2765, Dec. 1995.

[60] Z. Ma and E. Yamashita, “Comparative studies of discontinuities in single and double layered conductor-backed coplanar waveguides,” in *IEEE MTT-S Int. Microw. Symp. Dig.*, San Francisco, USA, Jun. 1996, pp. 1803–1806.

[61] M. Hotta, Y. Qian, and T. Itoh, “Efficient FDTD analysis of conductor-backed CPW’s,” *IEEE Trans. Microw. Theory Tech.*, vol. 47, no. 8, pp. 1585–1587, Aug. 1999.

[62] M. Hotta, M. Kobayashi, T. Inoue, and M. Hano, “Effects of backside grooving on leakage loss of conductor-backed coplanar waveguide,” in *Proc. Asia-Pacific Microw. Conf.*, Taipei, Taiwan, Dec. 2001, pp. 847–850.

[63] Y. Liu, C.-Y. Lee, and T. Itoh, “Slotline antenna with non-leaky coplanar (NLC) waveguide feed,” in *IEEE AP-S Int. Symp. Dig.*, Newport Beach, USA, Jun. 1995, pp. 366–369.

[64] H.-C. Liu, T.-S. Horng, and N. G. Alexopoulos, “Radiation of printed antennas with a coplanar waveguide feed,” *IEEE Trans. Antennas Propag.* , vol. 43, no. 10, pp. 1143–1148, Oct. 1995.

[65] Y. Qian and T. Itoh, “Characterization and minimization of mutual coupling between NLC-fed slot antennas,” in *IEEE MTT-S Int. Microw. Symp. Dig.*, Denver, USA, Jun. 1997, pp. 1623–1626.

[66] D. R. Jahagirdar and R. D. Stewart, “Nonleaky conductor-backed coplanar waveguide-fed rectangular microstrip patch antenna,” *IEEE Microw. Guided Wave Lett.*, vol. 8, no. 3, pp. 115–117, Mar. 1998.

[67] J. P. Jacobs, “Low-profile CPW-fed slot antenna with parasitic slot on conductor-backed two-layer substrate,” in *Proc. Int. Conf. Electromagn. Adv. Applicat.*, Torino, China, Sep. 2009, pp. 655–657.

[68] K.-P. Ma, J. Kim, F.-R. Yang, Y. Qian, and T. Itoh, “Leakage suppression in stripline circuits using a 2-D photonic bandgap lattice,” in *IEEE MTT-S Int. Microw. Symp. Dig.*, Anaheim, USA, Jun. 1999, pp. 73–76.

[69] F.-R. Yang, K.-P. Ma, Y. Qian, and T. Itoh, “A uniplanar compact photonic-bandgap (UC-PBG) structure and its applications for microwave circuits,” *IEEE Trans. Microw. Theory Tech.*, vol. 47, no. 8, pp. 1509–1514, Aug. 1999.

[70] K.-H. Oh, T.-Y. Kim, S. Moon, H.-J. Song, W.-B. Kim, C.-S. Park, and J.-I. Song, “Characterization of uniplanar compact photonic-bandgap finite-width conductor-backed coplanar waveguide by using an electrooptic near-field

mapping technique," *IEEE Trans. Microw. Theory Tech.*, vol. 54, no. 2, pp. 854–860, Feb. 2006.

[71] J. D. Shumpert, W. J. Chappell, and L. P. B. Katehi, "Parallel-plate mode reduction in conductor-backed slots using electromagnetic bandgap substrates," *IEEE Trans. Microw. Theory Tech.*, vol. 47, no. 11, pp. 2099–2104, Nov. 1999.

[72] R. Abhari and G. V. Eleftheriades, "Suppression of the parallel-plate noise in high-speed circuits using a metallic electromagnetic band-gap structure," in *IEEE MTT-S Int. Microw. Symp. Dig.*, Seattle, USA, Jun. 2002, pp. 493–496.

[73] F. Elek, R. Abhari, and G. V. Eleftheriades, "A uni-directional ring-slot antenna achieved by using an electromagnetic band-gap surface," *IEEE Trans. Antennas Propag.*, vol. 53, no. 1, pp. 181–190, Jan. 2005.

[74] J.-H. Chen, S.-Y. Chen, and P. Hsu, "Leakage-reduced conductor-backed coplanar waveguide with periodic structures and its antenna application," *IEEE Trans. Antennas Propag.*, vol. 59, no. 6, pp. 2078–2086, Jun. 2011.

[75] J. Hesselbarth and R. Vahldieck, "Leakage suppression in coplanar waveguide circuits by patterned backside metallization," in *IEEE MTT-S Int. Microw. Symp. Dig.*, Anaheim, USA, Jun. 1999, pp. 871–874.

[76] D. B. Schlieter and R. M. Henderson, “Designing high impedance etched ground GCPW,” in *Proc. IEEE 10th Annu. Wireless Microw. Technol. Conf.*, Clearwater, USA, Apr. 2009.

[77] T. Nishino, Y. Yoshida, Y. Suehiro, S.-S. Lee, K. Miyaguchi, T. Fukami, H. Oh-hashi, and O. Ishida, “A hollow-GCPW (HGCPW) as low-loss and wafer-conductivity-free structure on a single silicon wafer,” in *Proc. 33th European Microw. Conf.*, Munich, Germany, Oct. 2003, pp. 41–44.

[78] F. R. Williams and T. G. Ruttan, “Coplanar transmission structure having spurious mode suppression,” U.S. Patent 5 225 796, July 6, 1993.

[79] S.-J. Kim, H.-S. Yoon, and H.-Y. Lee, “Suppression of leakage resonance in coplanar MMIC package using a Si sub-mound Layer,” *IEEE Trans. Microw. Theory Tech.*, vol. 48, no. 12, pp. 2664–2669, Dec. 2000.

[80] W. Menzel and W. Grabherr, “A microstrip patch antenna with coplanar feed line,” *IEEE Microw. Guided Wave Lett.*, vol. 1, no. 11, pp. 340–342, Nov. 1991.

[81] Y. Turki, C. Migliaccio, and J.M. Laheurte, “Circularly polarised square patch antenna fed by coplanar waveguide,” *Electron. Lett.*, vol. 33, no. 15, pp. 1321–1323, Jul. 1997.

[82] K. Hettak and G. Delisle, “A novel antenna configuration for millimeter wave communication systems,” in *Proc*. *IEEE AP-S Int. Symp.*, Atlanta, USA, Jun. 1998, pp. 2092–2095.

[83] M. Boulmalf and G. Y. Delisle, “CPW fed microstrip antenna for indoor broadband wireless communications,” in *Proc*. *IEEE AP-S Int. Symp.*, Atlanta, USA, Jun. 1998, pp. 802–805.

[84] L. Giauffret and J.-M. Laheurte, “Parametric study of the coupling aperture in CPW-fed microstrip antennas,” *Proc*. *Inst. Elect. Eng.-Microw. Antennas Propag.*, vol. 146, no. 3, pp. 169–174, Jun. 1999.

[85] C.-Y. Huang and K.-L. Wong, “Coplanar waveguide-fed circularly polarized microstrip antenna,” *IEEE Trans. Antennas Propag.*, vol. 48, no. 2, pp. 328–329, Feb. 2000.

[86] C.-C. Hsu, P. Hsu, and J.-F. Kiang, “Analysis of coplanar waveguide-fed circular patch antenna,” in *Proc. Asia-Pacific Microw. Conf.*, Taipei, Taiwan, Dec. 2001, pp. 1338–1341.

[87] K. H. Y. Ip and G. V. Eleftheriades, “A compact CPW-based single-layer injection-locked active antenna for array applications,” *IEEE Trans. Microw. Theory Tech.*, vol. 50, no. 2, pp. 481–486, Feb. 2002.

[88] C.-Y. Huang and C.-W. Ling, “CPW feed circularly polarised microstrip antenna using asymmetric coupling slot,” *Electron. Lett.*, vol. 39, no. 23, Nov. 2003.

[89] I-J. Chen, C.-S. Huang, and P. Hsu, “Circularly polarized patch antenna array fed by coplanar waveguide,” *IEEE Trans. Antennas Propag.*, vol. 52, no. 6, pp. 1607–1609, Jun. 2004.

[90] I-J. Chen, “CPW-fed circularly polarized 2×2 sequentially rotated patch antenna array,” in *Proc. Asia-Pacific Microw. Conf.*, Suzhou, China, Dec. 2005.

[91] G. Mansour, P. S. Hall, P. Gardner, and M.K.A. Rahim, “Switchable multi-band coplanar antenna,” in *Proc. Loughborough Antennas Propag. Conf.*, Loughborough, UK, Nov. 2011, pp. 1–4.

[92] H. A. Elsadek, “CLIP antenna for wireless Bluetooth applications,” *IEEE Antennas Propag. Mag.*, vol. 47, no. 3, pp. 149–153, Jun. 2005.

[93] S. Chaimool, P. Akkaraeakthalin, and M. Krairksh, “CPW-fed slot antennas using loading metallic strips and a widened tuning stub with a finite reflector,” in *Proc. Int. Symp.Commun. Inform. Technol.*, Bangkok, Thailand, Oct. 2006, pp. 791–794.

[94] S.-Y. Chen, I-C. Lan, and P. Hsu, “In-line series-feed collinear slot array fed by a coplanar waveguide,” *IEEE Trans. Antennas Propag.*, vol. 55, no. 6, pp. 1739–1744, Jun. 2007.

[95] P. Cao, Y. Huang, J. Zhang, and Y. Lu, “A comparison of planar monopole antennas for UWB applications,” in *Proc*. *Loughborough Antennas Propag. Conf.*, Loughborough, UK, Nov. 2011, pp. 1–4.

[96] S.-P. Pan, J.-Y. Sze, and P.-J. Tu, “Circularly polarized square slot antenna with a largely enhanced axial-ratio bandwidth,” *IEEE Antennas Wireless Propag. Lett.*, vol. 11, pp. 969–972, 2012.

[97] G. Li, H. Zhai, L. Li, C. Liang, “A nesting-L slot antenna with enhanced circularly polarized bandwidth and radiation,” *IEEE Antennas Wireless Propag. Lett.*, vol. 13, pp. 225–228, 2014.

[98] D. Sievenpiper, L. Zhang, R. F. J. Broas, N. G. Alexopolous, and E. Yablonovitch, “High-impedance electromagnetic surfaces with a forbidden frequency band,” *IEEE Trans. Microw. Theory Tech.*, vol. 47, no. 11, pp. 2059–2074, Nov. 1999.

[99] F. Yang and Y. Rahmat-Samii, *Electromagnetic Band-Gap Structures in Antenna Engineering*. Cambridge, U.K.: Cambridge Univ. Press, 2009, pp. 4–6.

[100] S. Zhu and R. Langley, “Dual-band wearable antennas over EBG substrate,” *Electron. Lett.*, vol. 43, no. 3, pp. 141–142, Feb. 2007.

[101] K. Payandehjoo and R. Abhari, “Suppression of substrate coupling between slot antennas using electromagnetic bandgap structures,” in *Proc. IEEE AP-S Int. Symp.*, San Diego, USA, Jul. 2008.

[102] S. Zhu and R. Langley, “Dual-band wearable textile antenna on an EBG substrate,” *IEEE Trans. Antennas Propag.*, vol. 57, no. 4, pp. 926–935, Apr. 2009.

[103] K. Payandehjoo and R. Abhari, “Employing EBG structure in multiantenna systems for improving isolation and diversity gain,” *IEEE Antennas Wireless Propag. Lett.*, vol. 8, pp. 1162–1165, 2009.

[104] M. Mantash, A.-C. Tarot, S. Collardey, and K. Mahdjoubi, “Dual-band CPW-fed G-antenna using an EBG structure,” in *Proc. Loughborough Antennas Propag. Conf.*, Loughborough, UK, Nov. 2010, pp. 453–456.

[105] D.-N. Cui, Y.-A. Liu, S.-L. Li, and C.-P. Yu, “UC-EBG on reflector for 3.45-GHz frequency band antenna array application,” in *Proc. 2nd Pacific-Asia Conf. Circuits, Commun. and System*, Beijing, China, Aug. 2010, pp. 363–365.

[106] J. Joubert, J. C. Vardaxoglou, W. G. Whittow, and J. W. Odendaal, “CPW-fed cavity-backed slot radiator loaded with an AMC reflector,” *IEEE Trans. Antennas Propag.*, vol. 60, no. 2, pp. 735–742, Feb. 2012.

[107] M.-H. Hsu, T.-C. Tang, and K.-H. Lin, “EBG reflector-backed MIMO antenna with wideband isolation and uni-directional radiation pattern MIMO antenna for MIMO radar,” in *Proc*. *IEEE AP-S Int. Symp.*, Orlando, USA, Jul. 2013, pp. 612–613.

[108] V. V. Yem and B. Journet, “Novel high gain and broadband CPW-fed antennas with EBG for ITS applications,” in *Proc*. *Int. Conf. Adv. Technol. Commun.*, Ho Chi Minh City, Vietnam, Oct. 2013, pp. 451–456.

[109] P. Prakash, M. P. Abegaonkar, A. Basu, and S. K. Koul, “Gain enhancement of a CPW-fed monopole antenna using polarization-insensitive AMC structure,” *IEEE Antennas Wireless Propag. Lett.*, vol. 12, pp. 1315–1318, 2013.

[110] M.S. Alam, M.T. Islam, and N. Misran, “Inverse triangular-shape CPW-fed antenna loaded with EBG reflector,” *Electron. Lett.*, vol. 49, no. 2, pp. 86–88, Jan. 2013.

[111] D. M. Pozar, “Considerations for millimeter wave printed antennas,” *IEEE Trans. Antennas Propag.*, vol. AP-31, no. 5, pp. 740–747, Sep. 1983.

[112] R. L. Rogers and D. P. Neikirk, “Use of broadside twin element antennas to increase efficiency on electrically thick dielectric substrates,” *Int. J. Infrared Millim. Waves*, vol. 9, no. 11, pp. 949–969, 1988.

[113] R. L. Rogers and D. P. Neikirk, “Radiation properties of slot and dipole elements on layered substrates,” *Int. J. Infrared Millim. Waves*, vol. 10, no. 6, pp. 697–728, 1989.

[114] R. L. Rogers, S. M. Wentworth, D. P. Neikirk, and T. Itoh, “A twin slot antenna on a layered substrate coupled to a microstrip feed line,” *Int. J. Infrared Millim. Waves*, vol. 11, no. 10, pp. 1225–1249, 1990.

[115] S. M. Wentworth, R. L. Rogers, J. G. Heston, D. P. Neikirk, and T. Itoh, “Millimeter wave twin slot antennas on layered substrates,” *Int. J. Infrared Millim. Waves*, vol. 11, no. 2, pp. 111–131, 1990.

[116] J. G. Heston, S. M. Wentworth, R. L. Rogers, D. P. Neikirk, and T. Itoh, “MM wave/FIR twin slot antenna structures,” in *IEEE AP-S Int. Symp. Dig.*, Dallas, USA, May 1990, pp. 788–790.

[117] I-C. Lan and P. Hsu, “Parallel-plate slot array fed by conductor-backed coplanar waveguide,” in *Proc. 35th European Microw. Conf.*, Paris, France, Oct. 2005, pp. 473–476.

[118] I-C. Lan and P. Hsu, “Gain-enhanced slot antenna fed by conductor-backed coplanar waveguide,” in *Proc. Asia-Pacific Microw. Conf.*, Yokohama, Japan, Dec. 2006, pp. 73–76.

[119] I-C. Lan, S.-Y. Chen, and P. Hsu, “Coupled twin slots fed by conductor-backed coplanar waveguide,” *IEEE Trans. Antennas Propag.*, vol. 56, no. 6, pp. 1784–1786, Jun. 2008.

[120] I-C. Lan, S.-Y. Chen, and P. Hsu, “Pattern smoothness and gain enhancement of finite ground slot dipole antenna fed by conductor-backed coplanar waveguide,” in *Proc. IEEE AP-S Int. Symp.*, San Diego, USA, Jul. 2008.

[121] C.-H. Lee, S.-Y. Chen, and P. Hsu, “Efficiency-enhanced and size-reduced coupled twin slots capacitively fed by conductor-backed coplanar waveguide,” *IEEE Antennas Wireless Propag. Lett.*, vol. 8, pp. 1033–1035, 2009.

[122] C.-H. Lee, I-C. Lan, S.-Y. Chen, and P. Hsu, “Coplanar waveguide-fed twin slot antenna with and without back conductor,” in *Proc. IEEE AP-S Int. Symp.*, San Diego, USA, Jul. 2008.

[123] J.-H. Chen, Y.-J. Lu, P. Hsu, and S.-Y. Chen, “CBCPW-fed side-plane patch antenna,” in *Proc. 38th European Microw. Conf.*, Amsterdam, the Netherlands, Oct. 2008, pp. 531–534.

[124] Yen-Ju Lu, I-C. Lan, S.-Y. Chen, and P. Hsu, “Finite-width conductor-backed coplanar waveguide-fed side-plane antenna,” in *Proc. IEEE AP-S Int. Symp.*, San Diego, USA, Jul. 2008.

[125] K. Li, C. H. Cheng, T. Matsui, and M. Izutsu, “Simulation and experimental study on coplanar patch and array antennas,” in *Proc*. *Asia-Pacific Microw. Conf*., Sydney, Australia, Dec. 2000.

[126] K. Li, C. H. Cheng, T. Matsui, and M. Izutsu, “Coplanar patch antennas: principle, simulation and experiment,” in *Proc*. *IEEE AP-S Int. Symp.*, Boston, USA, Jul. 2001, pp. 402–405.

[127] K. Li and M. Izutsu, “Photodetection, photonic feeding coplanar patch antenna and transmitting experiment for radio-on-fiber system,” in *IEEE MTT-S Int. Microw. Symp. Dig.*, Phoenix, USA, May 2001, pp. 73–76.

[128] K. F. Tong, K. Li, T. Matsui, and M. Izutsu, “Wideband coplanar waveguide fed coplanar patch antenna,” in *Proc*. *IEEE AP-S Int. Symp.*, Boston, USA, Jul. 2001, pp. 406–409.

[129] P. L. Chin, A. Z. Elsherbeni, and C. E. Smith, “Characteristics of coplanar bow-tie patch antennas,” in *Proc*. *IEEE AP-S Int. Symp.*, San Antonio, USA, Jun. 2002, pp. 389–401.

[130] S. Pandey and R. Ramdadoss, “Coplanar patch antenna fed at the non-radiating edge,” in *Proc. IEEE AP-S Int. Symp.*, Monterey, USA, Jun. 2004, pp. 3397–3400.

[131] K. Li, C.-P. Chen, T. Anada, and T. Matsui, “Electric field in coplanar patch antenna (CPA) -- simulation and measurement --,” in *Proc*. *Asia-Pacific Microw. Conf.*, Suzhou, China, Dec. 2005.

[132] C.-H. K. Chin, Q. Xue, and C. H. Chan, “Design of a 5.8-GHz rectenna incorporating a new patch antenna,” *IEEE Antennas Wireless Propag. Lett.*, vol. 4, pp. 175–178, 2005.

[133] T. Zwick, D. Liu, J. Grzyb, and B. Gaucher, “A coplanar patch antenna for integration with mmWave SiGe Transceiver,” in *Proc*. *IEEE Int. Workshop Antenna Technol. Small Antennas Novel Metamaterials*, New York, USA, Mar. 2006, pp. 416–419.

[134] J.-H. Chen, S.-Y. Chen, and P. Hsu, “Conductor-backed coplanar waveguide fed circular coplanar patch antenna,” in *Proc*. *Asia-Pacific Microw. Conf.*, Yokohama, Japan, Dec. 2010, pp. 88–91.

[135] C. Kim, X. Cheng, D. E. Senior, K. T. Kim, and Y.-K. Yoon, “A surface micromachined high gain dielectric lens antenna for millimeter wave applications,” in *Proc*. *IEEE AP-S Int. Symp.*, Chicago, USA, Jul. 2012.

[136] Z. Du, A. Tamminen, J. Ala-Laurinaho, J. Saily, P. Rantakari, A. Luukanen, “Design and optimization of reconfigurable reflectarray element with MEMS

phase shifter," in *Proc. 7th European Conf. Antennas Propag.*, Gothenburg, Sweden, Apr. 2013, pp. 2422–2426.

[137] Z. N. Chen, N. Yang, Y.-X. Guo, and M. Y. W. Chia, "An investigation into measurement of handset antennas," *IEEE Trans. Instrum. Meas.*, vol. 54, no. 3, pp. 1100–1110, Jun. 2005.

[138] D. M. Pozar and B. Kaufman, "Comparison of three methods for the measurement of printed antenna efficiency," *IEEE Trans. Antennas Propag.*, vol. 36, no. 1, pp. 136–139, Jan. 1988.

[139] S. D. Rogers, "Electromagnetic-bandgap layers for broad-band suppression of TEM modes in power planes," *IEEE Trans. Microw. Theory Tech.*, vol. 53, no. 8, pp. 2495–2505, Aug. 2005.

[140] S. Shahparnia and O. M. Ramahi, "Electromagnetic interference (EMI) reduction from printed circuit boards (PCB) using electromagnetic bandgap structures," *IEEE Trans. Electromagn. Compat.*, vol. 46, no. 4, pp. 580–587, Nov. 2004.

[141] Y.-J. Lu and P. Hsu, "Design of an EBG-backed CPW-fed slot antenna," in *Proc. Asia-Pacific Microw. Conf.*, Kaohsiung, Taiwan, Dec. 2012, pp. 79–81.

[142] D. M. Pozar, *Microwave Engineering*, 3rd ed. New York, NY: Wiley, 2005, sec. 8.1.

[143] J. Liang, H.-Y. D. Yang, “Radiation characteristics of a microstrip patch over an electromagnetic bandgap surface,” *IEEE Trans. Antennas Propag.*, vol. 55, no. 6, pp. 1691–1697, Jun. 2007.

[144] K. C. Gupta, R. Garg, I. Bahl, and P. Bhartia, *Microstrip Lines and Slotlines*, 2nd ed. Boston, MA: Artech House, 1996, pp. 282–286.

[145] W. L. Stutzman, “Estimating directivity and gain of antennas,” *IEEE Antennas Propag. Mag.*, vol. 40, no. 4, pp. 7–11, Aug. 1998.

Publication List of Yen-Ju Lu

Journal Paper

[1] Y.-J. Lu, S.-Y. Chen, and P. Hsu, “A differential-mode wideband bandpass filter with enhanced common-mode suppression using slotline resonator,” *IEEE Microw. Wireless Compon. Lett.*, vol. 22, no. 10, pp. 503–505, Oct. 2012.

[2] Y.-W. Liu, Y.-J. Lu, and P. Hsu, “Harmonic suppressed slot loop antenna fed by coplanar waveguide,” *IEEE Antennas Wireless Propag. Lett.*, (accepted).

[3] Y.-J. Lu, Y.-W. Liu, and P. Hsu, “A hybrid design of printed antenna fed by coplanar waveguide with and without back conductor,” *IEEE Antennas Wireless Propag. Lett.*, (accepted).

International Conference Paper

[1] Y.-L. Shih, B.-H. Wang, Y.-J. Lu, J.-C. Cheng, S.-Y. Chen, and P. Hsu, “Capacitively-loaded loop antenna for multi-band mobile handsets,” in *Proc. IEEE Int. Workshop Antenna Technol.*, Chiba, Japan, Mar. 2008, pp. 239–242.

[2] Y.-J. Lu, I-C. Lan, S.-Y. Chen, and P. Hsu, “Finite-width conductor-backed coplanar waveguide-fed side-plane antenna,” in *Proc. IEEE AP-S Int. Symp.*, San Diego, USA, Jul. 2008.

[3] J.-H. Chen, Y.-J. Lu, P. Hsu, and S.-Y. Chen, “CBCPW-fed side-plane patch antenna,” in *Proc. 38th European Microw. Conf.*, Amsterdam, the Netherlands, Oct. 2008, pp. 531–534.

[4] Y.-J. Lu, S.-Y. Chen, and P. Hsu, “Finite-width conductor-backed coplanar waveguide-fed circularly polarized side-plane antenna,” in *Proc. IEEE AP-S Int. Symp.*, Toronto, Canada, Jul. 2010.

[5] Y.-J. Lu and P. Hsu, “Metamaterial-inspired circularly polarized slot dipole antenna fed by coplanar waveguide,” in *Proc. IEEE AP-S Int. Symp.*, Chicago, USA, Jul. 2012.

[6] Y.-J. Lu and P. Hsu, “Design of an EBG-backed CPW-fed slot antenna,” in *Proc. Asia-Pacific Microw. Conf.*, Kaohsiung, Taiwan, Dec. 2012, pp. 79–81.

[7] Y.-J. Lu and P. Hsu, “A dual-band CPW-fed stepped-impedance slot antenna with wide range of frequency ratio,” in *Proc. IEEE AP-S Int. Symp.*, Orlando, USA, Jul. 2013, pp. 936–937.

[8] Y.-J. Lu and P. Hsu, “A modified CPW-fed slot dipole antenna with wideband harmonic suppression,” in *Proc. IEEE Int. Workshop Electromagn.*, Sapporo, Japan, Aug. 2014, pp. 60–61.